Near-Highway Aerosol and Gas-phase Measurements in a High Diesel Environment

DeWitt H.L.[1], Hellebust S.[1], Temime-Roussel B.[1], Ravier S.[1], Polo L.[2,3], Jacob V.[2], Buisson C., Charron A.[3], André M.[3], Pasquier A.[3], Besombes J.L.[4], Jaffrezo J.L.[2], Wortham H.[1], Marchand N.[1]

[1]Aix Marseille Université, CNRS, LCE FRE 3416, 13331 Marseille, France
[2] Université Grenoble Alpes, CNRS, LGGE, F-38000 Grenoble, France
[3] IFSTTAR, Case 24, 69675 Bron Cédex, France
[4] Université de Savoie, LCME, 73376 Le Bourget du lac, France

Corresponding authors: H. Langley DeWitt (Helen-Langley.Dewitt@univ-amu.fr) and Nicolas Marchand (Nicolas.Marchand@univ-amu.fr).

Helen Langley DeWitt 2/28/15 2:35 PM
Deleted: Direct

Helen Langley DeWitt 2/28/15 2:35 PM
Deleted: of Near-Highway Emissions

Helen Langley DeWitt 2/28/15 2:35 PM
Formatted: French

Helen Langley DeWitt 2/28/15 2:35 PM
Formatted: French, Not Superscript/ Subscript

Helen Langley DeWitt 2/28/15 2:35 PM
Formatted: French

Helen Langley DeWitt 2/28/15 2:35 PM
Formatted: French

Helen Langley DeWitt 2/28/15 2:35 PM
Moved (insertion) [1]

Helen Langley DeWitt 2/28/15 2:35 PM
Formatted: French

Helen Langley DeWitt 2/28/15 2:35 PM
Deleted: .

Helen Langley DeWitt 2/28/15 2:35 PM
Formatted: French

Helen Langley DeWitt 2/28/15 2:35 PM
Moved up [1]: André M.

Helen Langley DeWitt 2/28/15 2:35 PM
Deleted: [3], Pasquier A[3]

Helen Langley DeWitt 2/28/15 2:35 PM
Formatted: English (US)

Abstract

Diesel-powered passenger cars currently outnumber gasoline-powered cars in many countries, particularly in Europe. In France, diesel cars represented 61% of light duty vehicles in 2011 and this percentage is still increasing (French Environment and Energy Management Agency, ADEME). As part of the September 2011 joint PM-DRIVE (Particulate Matter- DiRect and Indirect on-road Vehicular Emissions) and MOCOPO (Measuring and mOdeling traffic COngestion and POllution) field campaign, the concentration and high-resolution chemical composition of aerosols and volatile organic carbon (VOC) species were measured adjacent to a major urban highway south of Grenoble, France. Alongside these atmospheric measurements, detailed traffic data were collected from nearby traffic cameras and loop detectors, which allowed the vehicle type, traffic concentration, and traffic speed to be quantified. Six aerosol age and source profiles were resolved using the positive matrix factorization (PMF) model on real-time high-resolution aerosol mass spectra. These six aerosol source/age categories included a hydrocarbon-like organic aerosol (HOA) commonly associated with primary vehicular emissions, a nitrogen containing aerosol (NOA) with a diurnal pattern similar to that of HOA, oxidized organic aerosol (OOA), and biomass burning aerosol (BBOA). While quantitatively separating influence of diesel versus gasoline proved impossible, a low HOA: Black Carbon ratio, similar to that measured in other high-diesel environments, and high levels of NOx, also indicative of diesel emissions, were observed. Although the measurement site was located next to a large source of primary emissions, which are typically found to have low oxygen incorporation, OOA was found to comprise the majority of the measured organic aerosol, and isotopic analysis showed that the measured OOA contained mainly modern carbon, not fossil-derived carbon. Thus, even in this heavily vehicular-emission impacted environment, photochemical processes, biogenic emissions, and aerosol oxidation

Helen Langley DeWitt 2/28/15 2:35 PM
Deleted: Light Duty Vehicles

Helen Langley DeWitt 2/28/15 2:35 PM
Deleted: identification of

Helen Langley DeWitt 2/28/15 2:35 PM
Deleted: and characteristics, and

Helen Langley DeWitt 2/28/15 2:35 PM
Deleted: and compared to measured aerosol and VOCs.

Helen Langley DeWitt 2/28/15 2:35 PM
Deleted: the

Helen Langley DeWitt 2/28/15 2:35 PM
Deleted: A comparison between these high-diesel environment measurements and measurements taken in low-diesel (North American) environments was examined and the potential feedback between vehicular emissions and SOA formation was probed.

dominated the overall organic aerosol mass measured during most of the campaign.

1. Introduction

Aerosols are known to have adverse effects on human health and on the global climate. The World Health Organization (WHO) recently added anthropogenic aerosol and air pollution to their list of known carcinogens (WHO, 2013), and high mass concentrations of particles less than 2.5 micrometers in diameter (PM2.5), such as those emitted by vehicular combustion processes, are particularly harmful (Lighty et al., 2000). Vehicular traffic is a large source of submicrometer anthropogenic aerosol and proximity to large sources of vehicular emissions has been shown to increase lung and heart disease, especially in children (Brugge et al., 2007). A recent WHO report examined the toxilogical effects of black carbon (BC) aerosol, a known emission of diesel vehicles. Although no difference in toxicology between PM2.5 and BC aerosol inhalation was found, BC was cited as a marker for more general vehicular emissions, which have been shown to have negative health effects; diesel exhaust was added as a known carcinogen the year before general air pollution and PM2.5 (Janssen, World Health Organization, 2012). Aside from the potential detrimental health effects of BC, BC also has significant implications for climate change. Unlike the majority of aerosol (e.g., most organic aerosol, ammonium sulfate, ammonium nitrate), BC aerosol is associated with global warming due to its high absorption of solar radiation (Bond et al., 2013). Diesel vehicles have been singled out as important sources of BC to regulate as, unlike most other BC sources, diesel vehicles tend not to co-elute high concentrations of other, less absorbing (thus more cooling) aerosol and therefore have a higher net heating effect than mixed-emission black carbon sources (Bond et al., 2013).

In France, the lower cost of diesel fuel (due to a lower taxation rate of diesel fuel versus gasoline fuel) and the generally higher fuel efficiency of diesel engines have increased the popularity of diesel passenger cars. In 2011, 82% of the fuel consumed in France was diesel (World Bank, 2011). For comparison, this percentage in 2011 was 28% in the US, 57% in China, 70% in the European Union,

Helen Langley DeWitt 2/28/15 2:35 PM
Deleted: For vehicular aerosol emissions, factors such as the fuel used (diesel versus gasoline), age of the car engine, and highway speed (stop and go traffic versus constant speed) can affect the concentration and physical and chemical composition of the aerosol emitted.

Helen Langley DeWitt 2/28/15 2:35 PM
Deleted: caused

Helen Langley DeWitt 2/28/15 2:35 PM
Deleted: to outnumber gasoline passenger cars: in 2011 diesel cars represented 60% of the total vehicular fleet (Light Duty Vehicles, LDV) (61% in 2013) according to the French Environment and Energy Management Agency (ADEME). The influence of diesel vehicles increases if we consider the total fuel consumption per capita, which better captures the use of diesel and gasoline vehicles on the road (road sector only, World Bank, 2011).

115 49% in Latin America and the Middle East, and 83% in low-income countries.

116 The emission characteristics and emission limits of these two types of engines (diesel and
117 gasoline) are quite different: diesel vehicles have higher emission factors for primary organic aerosol
118 (POA) and BC, while gasoline-powered vehicles have higher emission factors for carbon monoxide
119 (CO), carbon dioxide (CO_2), and volatile organic carbon (VOCs) (e.g., trimethylbenzene, benzene)
120 (Platt et al., 2013). Black carbon, in particular, is closely associated with diesel: in Europe, North
121 America, and Latin America, an estimated 70% of BC emissions are from diesel-powered vehicles
122 (Bond et al., 2013). These differences in emissions were observed in studies performed in Mexico City,
123 where particulate and VOC emissions were measured both at stationary measurement sites and during
124 vehicular chases with the Aerodyne Mobile Laboratory (Thornhill et al., 2010). During this study,
125 diesel and gasoline vehicles on the road were manually counted and specific vehicles were followed
126 and their emissions captured. From these data, diesel was found to contribute almost all of the BC
127 mass and particle number concentration, along with the majority of PM2.5, while gasoline emissions
128 were found to have elevated levels of toluene and benzene (Thornhill et al., 2010). In Marseille,
129 France, a traffic tunnel experiment measured an organic carbon/elemental carbon ratio (OC/EC) in
130 PM2.5 of 0.3-0.4, which indicates that significant amounts of black carbon is emitted from local traffic
131 in Marseille (El Haddad et al., 2009). Recent measures have been taken in Europe to reduce the
132 particulate emission from diesel vehicles: from Euro 4 to Euro 5, a diesel particle filter (DPF) was
133 introduced in diesel vehicles and the regulated emission limit for PM2.5 was halved for diesel cars and
134 trucks.

135 Aerosol and VOC emissions from both vehicle types, as well as biogenic emissions, industrial
136 emissions, and emissions from other sources, will react together in the atmosphere and potentially form
137 secondary organic aerosol (SOA). Thus, primary aerosol emissions may not be the most important
138 emission factor to take into account for global reduction in anthropogenic aerosol. After emission,
139 VOCs can react in the atmosphere and form SOA. From these reactions, gasoline VOC emissions could

Helen Langley DeWitt 2/28/15 2:35 PM
Deleted: rates

Helen Langley DeWitt 2/28/15 2:35 PM
Deleted: rates

Helen Langley DeWitt 2/28/15 2:35 PM
Deleted: toluene

Helen Langley DeWitt 2/28/15 2:35 PM
Deleted: Outside of smog-chamber studies, both aerosol

ultimately lead to the formation of higher concentrations of organic aerosol than organic aerosol released directly from diesel vehicles, as reported in a recent study comparing the SOA formation from a Euro 3 diesel LDV and a Euro 5 gasoline LDV (Platt et al., 2013).

A recent study by Bahreini et al. (2012) measured similar levels of SOA in the heavily traffic-influenced LA Basin during both weekend and weekday afternoons. While diesel-powered vehicle numbers on the road decrease significantly on the weekends in the LA area, the measured SOA does not, which leads to the conclusion that gasoline emissions are more responsible for SOA than diesel emissions (Bahreini et al., 2012). Nordin et al. (2013) performed smog-chamber studies on SOA formation from gasoline-vehicle VOC emissions during simulated cold start and idling driving conditions, and confirmed the high potential of SOA formation from gasoline car exhaust. Another recent paper calculates the reactivity potential of diesel and gasoline fuel and comes to the opposite conclusion: that due to the reactivity potential of diesel fuel, diesel-powered vehicles should contribute greater amounts of SOA than gasoline-powered vehicles to the atmosphere (Gentner et al., 2012). Thus, controversy still exists regarding the eventual aerosol emission factors of diesel and gasoline engines when considering both primary emissions and potential SOA formation.

Finally, gas-phase NO and NO_2 (NOx) ambient concentrations are also mostly associated with diesel fuel use (Vestreng et al., 2009). Throughout Europe, while NOx emission standards for diesel vehicles have increased in stringency in recent years, ambient NO_2 levels have not shown a corresponding decrease (Vestreng et al., 2009). The reduction of atmospheric NOx is important for health-related reasons as an increase in NOx leads to an increase in tropospheric ozone, which is a known lung irritant. NOx levels have also been shown to affect the formation rate, formation pathways, and chemical composition of secondary organic aerosol from the reaction of primary species in numerous chamber studies (Carlton et al., 2009; Kroll et al., 2005; Ng et al., 2007, 2008; Presto et al., 2010).

European vehicular emissions, near-highway pollution levels, and the chemical composition of

Helen Langley DeWitt 2/28/15 2:35 PM
Deleted: Smog chamber measurements and field studies on vehicular emissions are important as differences in the SOA formation potential of diesel and gasoline gas- and particle-phase emissions are not fully understood.

Helen Langley DeWitt 2/28/15 2:35 PM
Deleted: They show that after a cumulative OH exposure of ~5 × 10^6 cm^{-3} h^{-1}, the formed SOA was 1–2 orders of magnitude higher than the primary OA emissions.

highway pollution may be quite different than those measured in North America due to many factors, including: 1) different emission standards and fuel regulations in the two regions 2) different after-treatment devices to reduce the emission of certain pollutants and 3) a much larger percentage of diesel-powered passenger cars on the road. A comparison between European and North American near-highway measurements could lead to further understanding of the effects of diesel versus gasoline on near-highway atmospheric chemistry.

To fully categorize the aerosol, VOC, and NOx emissions of traffic in France, the joint PM-DRIVE (Particulate Matter- DiRect and Indirect on-road Vehicular Emissions) and MOCOPO (Measuring and mOdeling traffic COngestion and POllution) field mission took place in the Grenoble basin, France during the fall of 2011 at a near-highway location south of the city center. During the field measurements discussed in this paper, traffic cameras allowed vehicle type determination through license plate automatic identification. Traffic densities, speed and total flow were quantified through loop detectors, while measurements of the chemical composition, concentration, and size of aerosol were collected using both real-time and offline analysis, and parallel data on the gas-phase chemical composition of the roadway-adjacent environment were also collected. A source apportionment model was applied to real-time aerosol chemical composition data. Particular attention was paid to the chemical composition of particles and VOCs emitted during morning and evening rush hours in an attempt to elucidate the primary vehicular influence on near-highway air pollution.

2. Experimental Methods

2.1. Description of the Measurement Site

The sampling site was located at 45.150641 N, 5.726028 E (Figure 1), just south of Grenoble, France adjacent to a major highway (south of E712, with A480 2 km to the east). During the week, the total traffic on the highway was about 95,000 vehicles day^{-1} (65,000 during the weekend). Grenoble, a large city with over half a million people, is located in the southeast of France at the foothills of the Alps. The surrounding mountain ranges both buffer the Grenoble area from the effects of transported

Helen Langley DeWitt 2/28/15 2:35 PM
Deleted: These measurements were part of a larger campaign that including direct tail-pipe emission measurements and smog chamber studies.

Helen Langley DeWitt 2/28/15 2:35 PM
Deleted: the

Helen Langley DeWitt 2/28/15 2:35 PM
Deleted: and traffic

Helen Langley DeWitt 2/28/15 2:35 PM
Deleted: East

aerosol and can also trap pollution within the valley, particularly during the winter months and periods of temperature inversions. The isolating effect of the mountains thus simplifies the potential sources for aerosol, making it an interesting location for the study of specific aerosol emission sources.

2.2. Traffic Cameras and Loop Detectors

Traffic cameras mounted to a roadway sign were used to capture the license plate numbers of vehicles driven on the highway close to the field measurement site. These numbers were later used to classify vehicular traffic into different categories: vehicle type (LDV, Heavy duty vehicles (HDV), buses) and age, vehicle size and engine capacity, fuel type (diesel or gasoline), and Euro number (i.e. the pollutant emission regulation that the vehicle complies with), The speed of the passing vehicles was also monitored with the classical traffic detector (double electromagnetic loops, able to identify the passing of all vehicles and their speeds), which allowed the identification of periods of stop-and-go, dense, or free-flow traffic.

2.3. Massalya Platform

The MASSALYA platform is a mobile laboratory equipped for air quality measurements with a hub located at the Aix Marseille Université. For the field campaign, PM2.5 and PM1 sampling heads situated above the roof of the stationary truck were connected to a variety of online instrumentation located within the truck body. Complementary off-line analysis was performed on filter samples collected by HiVol samplers located adjacent to the MASSALYA platform. All sampling occurred approximately 15 m from one of the traffic lines, as shown in Figure 1. Further details can be found in Polo-Rehn, (2013).

Helen Langley DeWitt 2/28/15 2:35 PM
Deleted: .

A High-Resolution Time-of-Flight Aerosol Mass Spectrometer (Aerodyne, HR-ToF-AMS) was used to analyze the chemical composition, size, and concentration of non-refractory submicrometer particles in the ambient atmosphere (DeCarlo et al., 2006). Instrument specifications have been discussed in detail elsewhere (DeCarlo et al., 2006). Briefly, both high resolution and size-speciated chemical information for ambient aerosol were obtained from this instrument. Aerosols were

238 vaporized at 600 ^{o}C, ionized using electron ionization (EI) at an energy of 70 eV, and the chemical
239 composition of bulk aerosol was measured using a ToF mass spectrometer (TOFWERK). Aerosol
240 spectra were continuously collected and a two-minute average spectrum was obtained. Aerosol
241 vacuum aerodynamic diameter was calculated by setting a particle start time using a chopper wheel
242 and measuring the particle flight time along the particle ToF (pToF) sizing region (DeCarlo et al.,
243 2006). Typical resolution during the campaign was around 2800 m/Δm (where m=*m/z* and Δm=full-
244 width at half max of the mass peak).
245 In addition to the HR-ToF-AMS, a Size-Mobility Particle Scanner (TSI, SMPS) was used to
246 measure the size distribution and concentration of ambient aerosol and a Multiangle Absorption
247 Photometer (Thermofischer, MAAP 5012) was used to measure the concentration of black carbon.
248 High resolution mass spectra of VOCs were obtained using an Ionicon Proton-Transfer
249 Reaction Time of Flight Mass Spectrometer 8000 (PTR-ToF-MS, hereafter referred to as PTR-MS)
250 (Graus et al., 2010). The PTR-MS analyzes trace (parts per trillion by volume) VOCs with high mass
251 resolution, which allows the separation of different species with the same nominal mass and the
252 identification of each peak's elemental formula. The PTR-MS was run with a 25 second time
253 resolution and a flow of 100 cm^3 min^{-1}. Drift tube parameters of the PTR-MS were as follows:
254 Voltage: 560 V, Drift tube pressure: 2.11 mbar, Drift tube temperature: 333 K, resulting in an E/N
255 (electric field/number concentration of neutral particles) of 133 Td.
256 The SMPS, PTR-ToF-MS, and HR-ToF-AMS were connected to the same sample inlet with a
257 PM2.5 sampling head and a sample flow of 1 m^3 hr^{-1}. Particles were dried (RH<30%) using a Nafion
258 dryer prior to measurement with the HR-ToF-AMS and SMPS. The MAAP was connected to a
259 separate PM1 sampling head. PM1 filter HiVol (30 m^3 h^{-1}) samples were collected on quartz filters
260 (Tissuquartz) on a daily basis and analyzed for radiocarbon isotope data. Radiocarbon measurements
261 were conducted using ARTEMIS Accelerator Mass Spectrometry, at Saclay (CNRS-CEA-IRD-IRSN,
262 France) on the total carbon (TC) fraction after a combustion of the samples at 850°C. The method is

Helen Langley DeWitt 2/28/15 2:35 PM
Deleted: .

fully described in El Haddad et al. (2011).

A Young meteorological station was also installed to capture wind speed, wind direction, relative humidity, and temperature data at the measurement location.

2.4. Air Rhône Alpes station

Twenty meters east of the Massalya platform, still adjacent to the highway, the Air Rhône Alps station collected PM2.5 HiVol (30 m^3 h^{-1}) samples on quartz fiber filters (Tissuquartz) with a time resolution of 4 hours. PM2.5 samples were analyzed for EC/OC, inorganic ions, and targeted organic tracers (Polo-Rehn, 2013).

Organic compounds in these PM samples were also quantified by gas chromatography coupled with mass spectrometry (GC-MS), following the method detailed in El Haddad et al. (2009) and Favez et al. (2010). EC and OC measurements were performed using the Thermo-Optical Transmission (TOT) method on a Sunset Lab analyzer (Birch and Cary, 1996; Jaffrezo et al., 2005) following the EUSAAR2 temperature program (Cavalli et al., 2010). Ionic species were analyzed with Ionic Chromatography (IC) following the method described in Jaffrezo et al. (1998).

All filters used in this study were preheated at 500 °C during 3 h. Samples were stored at -18 °C in aluminum foil and sealed in polyethylene bags until analysis.

In addition, NOx (NO and NO_2), PM10 and PM2.5 mass concentrations were measured and a Tapered Element Oscillating Microbalance equipped with a Filter Dynamic Measurement System (TEOM-FDMS, Thermo Scientific) for real-time measurements of PM10 and PM2.5.

3. Results and Discussion

3.1 Traffic Conditions at the Measurement Site

A detailed view of the measured traffic is presented in the supplementary information (Figure S1). Briefly, the overall makeup of the traffic remained fairly steady throughout the campaign. The

Helen Langley DeWitt 2/28/15 2:35 PM
Deleted: meter to the East along

Helen Langley DeWitt 2/28/15 2:35 PM
Deleted: . The correlation of diesel and gasoline vehicles (data averaged for 15 minutes) and four hour averages

Helen Langley DeWitt 2/28/15 2:35 PM
Deleted: vehicle type (LDV, HDV, and buses) and Euro number of passing vehicles are shown

Helen Langley DeWitt 2/28/15 2:35 PM
Deleted: 2A and B, respectively. The

Helen Langley DeWitt 2/28/15 2:35 PM
Deleted: LDVs accounted for the majority of traffic (94%) and only experienced a small drop-off in flow over the weekends (87% of the weekday flow). HDVs and buses, however, were present in much higher concentrations during the week versus the weekend (2.7 times less buses and HDVs on the weekends), and also were in lower numbers on the road during the early morning and late evening hours. The ratio of LDVs to HDVs increased by a factor of 4 from the morning rush hour peak to the evening rush hour peak.

bulk of the vehicles directly affecting the measurement site were Euro 4 (released in 2005) or older; thus, the most recent emission regulations had only a small effect on the air quality around the field site. The ratio between diesel and gasoline cars was found to be 2.6, or 72% diesel, with a high correlation (R^2=0.96) between diesel and gasoline vehicles.

3.2. General atmospheric conditions and aerosol and VOC concentrations and evolution

Wind speeds were generally low throughout the campaign (<1-2 m/s) with higher wind speeds peaking in the afternoons and tapering off in the evenings. The wind direction was primarily from the northwest, from the direction of the nearby highway. A diagram of the two measurement stations, the wind rose plot for the Massalya location, and polar plots showing the concentration of NO and BC as a function of wind direction are shown in Figure 1. BC and NO were associated with all wind directions, though slightly higher from the highway direction, which suggested that the measurement site was directly and strongly influenced by the traffic emissions. However, in order to bett

er describe the traffic influence, we defined high traffic periods (HT) within the dataset. These HT periods were selected as follows : wind direction >40 or <320, NO in the 75th percentile, and from 6:30-9:30 or 17:00-20:00 (rush hour periods). The fixed location of the measurement stations made determination of concentration drop-off as a function of distance from the roadway impossible to determine with the dataset, although that has been shown to be important in other studies (such as Karner et al., 2010). However, the measurements were all taken closer to the roadway (~15 m) than the calculated distance where roadway emission drop off to background levels (115-570 m, Karner et al., 2010).

The campaign time series concentration of submicrometer non-refractory aerosol sulfate (SO_4), ammonium (NH_4), nitrate (NO_3), and organic species from the HR-ToF-AMS is shown in Figure 2A. The limit of detection for each species was calculated using the method described byDeCarlo et al. (2006) and found to be 0.30, 0.21, 0.06, and 0.33 μg m^{-3} for SO_4, NH_4, NO_3, and organic aerosol, respectively, for our measurements with a time resolution of 2.5 min. A collection efficiency (CE) of

Helen Langley DeWitt 2/28/15 2:35 PM
Deleted: From the 15 minute time-resolution traffic data (not shown), approximately five times as many Euro 4 as Euro 5 cars were counted on the road during the measurement period, while similar numbers of Euro 3 and Euro 4 cars were observed. A relatively high correlation

Helen Langley DeWitt 2/28/15 2:35 PM
Deleted: the different Euro classifications of vehicles was observed (R^2 values of 0.7 for Euro 5 and Euro 4, 0.9 for Euro 3 and Euro 4, using 15 minute time resolution traffic data). For diesel cars, from Euro 4 (released in 2005) to Euro 5 (released in 2009), NOx emission limits decreased from 0.25 to 0.18 g km^{-1} and particulate emission limits decreased from 0.025 to 0.005 g km^{-1}. From Euro 3 (released in 2000) to Euro 4 another two-fold decrease in NOx and PM emission limits was implemented for diesel vehicles. Gasoline NOx emission limits were reduced from 0.15 to 0.08 to 0.06 g km^{-1} from Euro 3 to Euro 5, and total hydrocarbon emission limits were reduced from 0.20 to 0.10 g km^{-1} from Euro 3 to Euro 4. No PM limits were implemented for gasoline-powered vehicles until Euro 5, where a limit of 0.005 g km^{-1} for direct-injection vehicles was introduced, and no total hydrocarbon emission limits have been introduced for diesel-powered vehicles.

Helen Langley DeWitt 2/28/15 2:35 PM
Deleted: on the highway was found (Figure 2B). The ratio between diesel and gasoline (the slope of the line) was found to be 2.6, or 72% diesel. This value is slightly higher than that reported by ADEME for French vehicle fleet (61%). However ADEME data represent the registered vehicles and not the on-road vehicles. This difference highlights most probably the combined effects of fuel costs and of vehicles consumption. Additionally, no weekly variation (weekend versus weekday) in the ratio of diesel: gasoline powered vehicles on the road was observed, unlike that commonly observed on North American highways (Bahreini et al., 2012).

Helen Langley DeWitt 2/28/15 2:35 PM
Deleted:

Helen Langley DeWitt 2/28/15 2:35 PM
Formatted: None

Helen Langley DeWitt 2/28/15 2:35 PM
Deleted: implying

Helen Langley DeWitt 2/28/15 2:35 PM
Deleted: station was most the time downstream from the highway.

Helen Langley DeWitt 2/28/15 2:35 PM
Deleted: 3A

0.75 was applied to HR-ToF-AMS aerosol concentration measurements taken during this campaign. The CE factor compensates for incomplete vaporization of non-refractory species due to particle bounce, the likelihood of which changes with particle phase and chemical speciation (Huffman et al., 2005; Matthew et al., 2008). This CE was calculated by comparing the HR-ToF-AMS SO_4 concentrations to 4 hour filter concentrations (Figure S2). This comparison gave a value of 0.75±0.03 for the slope between the two types of measurements.

PM2.5 averaged 17 μg m^{-3} for the campaign (Figure S3) while PM10 averaged 22 μg m^{-3}. These values increased slightly during HT periods (a 1.3 and 1.25x increase, respectively). Black carbon and organic aerosol species dominated the measured aerosol composition throughout the campaign, and comprised 39 and 40% of the total speciated submicrometer aerosol, respectively. PM2.5 had a somewhat higher mass variation than the AMS + BC measured mass (Figure S3), likely due to the smaller measurement size cutoff for AMS (1 μm) and the presence of road dust in the local environment, a large portion of which may be non-refractory and those unable to be measured by the AMS. Increases in BC and the aerosol marker *m/z* 57 ($C_4H_9^+$), a marker for primary organic carbon in the HR-ToF-AMS (Zhang et al., 2005), correlated in time to the observed morning and evening traffic peaks (Figure 2B), with BC levels reaching 10-16 μg m^{-3} during the mornings (Figure 2A) for 2.5 min averaged measurements. As expected, an increase of BC and m/z 57 (1.5x) was observed during HT periods. Note that BC concentrations during high filter loadings (BC accumulation rate > 0.14 μg min^{-1}) have been removed to compensate for the underestimation of BC by the MAAP during periods of high concentrations (Hyvärinen et al., 2013). Along with increased concentrations of *m/z* 57 and BC, elevated number concentrations of small particles (up to 1-2x10^5 cm^{-3} during peaks from daily base levels of 2-4x10^4 cm^{-3}) were observed during periods of HT (Figure 2D), for 5 min measurements. BC and *m/z* 57 had similar daily averages throughout the campaign; however, overall organic concentration rose significantly during the period from 9/12-9/14, when particle growth events were

Helen Langley DeWitt 2/28/15 2:35 PM
Deleted: nonrefractory

Helen Langley DeWitt 2/28/15 2:35 PM
Deleted: S1

Helen Langley DeWitt 2/28/15 2:35 PM
Deleted: S2

Helen Langley DeWitt 2/28/15 2:35 PM
Deleted: 3A), and comprised 39 and 40% of the total speciated submicrometer aerosol, respectively.

Helen Langley DeWitt 2/28/15 2:35 PM
Deleted: 3B

Helen Langley DeWitt 2/28/15 2:35 PM
Deleted: 3A

Helen Langley DeWitt 2/28/15 2:35 PM
Deleted: heavy traffic

Helen Langley DeWitt 2/28/15 2:35 PM
Deleted: 3D

observed (Figure 2D). The geometric number mode diameter rose over the course of each day to a maximum diameter each afternoon, when photochemical processing was the most intense. A marker for oxidized, aged organic aerosol (Figure 2C, *m/z* 44, COO^+) also rose in concentration during this time period, further confirming that the larger aerosol and higher organic mass concentrations were due to aging and secondary organic aerosol formation processes. A period of heavy rain on the 18th and 19th of September removed much of the organic aerosol from the local atmosphere. Black carbon concentrations and small particle concentrations quickly returned to their previous levels. A new accumulation period was observed after rainfall (Figure 2D), with the mode diameter of particles increasing as secondary aerosol was formed again. The slow rise of organic concentration during these periods, the lower BC:Org ratio, the enhancement of organic concentration outside of normal traffic periods, and the low level of NO during these accumulation periods all suggest that this increase in organic aerosol concentration was driven by regional influences, not by nearby vehicular emissions, and a more southerly wind direction during this time confirmed the transport of non-highway air masses to the measurement site.

These findings are similar to those presented recently by Sun et al., (2012), who measured aerosol size and chemical composition adjacent to the Long Island Expressway in New York and observed that traffic-influenced aerosol emissions were primarily small particles which varied in concentration with changes in traffic throughout the day. During periods with less traffic influence, more oxygenated organic aerosol (OOA) and inorganic ions with larger mode diameters and lower temporal variations were observed (Sun et al., 2012).

The time series concentrations of selected VOC peaks are shown in Figure 3. Primary traffic related VOC species, such as aromatics (benzene and trimethylbenzene), were found to have high temporal variations similar to those of traffic-related aerosol species and NOx (Figure 4C and D). NOx levels were often over 400 ppbv during the morning rush hours, while the PTRMS peak corresponding (in part) to toluene and benzene peaked around 2 to 1 ppbv (respectively). During a recent chamber

Helen Langley DeWitt 2/28/15 2:35 PM
Deleted: 3D

Helen Langley DeWitt 2/28/15 2:55 PM
Deleted: 3C

Helen Langley DeWitt 2/28/15 2:35 PM
Deleted: 3D

Helen Langley DeWitt 2/28/15 2:35 PM
Deleted: 4

Helen Langley DeWitt 2/28/15 2:35 PM
Deleted: toluene

study in Ispra, Italy, fresh diesel emissions PTR-MS VOC spectra were found to contain peaks with the same mass as $CH_4NO_2^+$ and $C_2H_5O^+$ (Hellebust et al., 2013, 2014), not present in fresh gasoline emissions. These same peaks were also observed during this work and found to vary with traffic during this measurement period, but had a smoother variation than the observed aromatics (Figure 3B). While this species is unique for fresh diesel emissions versus gasoline emissions, aging processes occur rapidly and other sources may contribute to this mass peak. Thus, these species, while increasing with traffic, cannot be assumed to be tracers for primary diesel emissions in particular; no high-concentration unique tracer peak for diesel VOC emissions was resolved from the fresh diesel emission spectra in these chamber experiments (Hellebust et al., 2015). A slight increase of the traffic related VOCs (1.2x for benzene and trimethylbenzene) was observed during HT periods compared to the campaign average. For $CH_4NO_2^+$ this relative increase during HT periods is lower (8%), which could confirm multiple sources of this compound.

In addition to traffic-related VOC emissions, mass peaks corresponding in exact mass to biogenic emissions, such as isoprene, were measured in ppbv levels. These peaks were found to rise in concentration with the ambient temperature (Figure 3A), typical of isoprene peaks. The presence of isoprene and its oxidation product, methyl vinyl ketone (MVK) or its isomer methacrolein (MACR), in similar concentrations as that of the major traffic-related VOC peaks (ppbv levels) suggested that biogenic emissions also significantly influenced the local atmosphere despite close proximity to anthropogenic emission sources (i.e., road traffic).

The high morning concentrations of traffic-related pollutants, compared to evening concentrations, were caused in part by a low early morning boundary layer that rose during the day and fell during the night. Boundary layer heights (BLH) were estimated using the Hybrid Single Particle Lagrangian Integrated Trajectory (HYSPLIT) backtrajectory model. The HYSPLIT model either extracts the BLH from meteorological file input into the model or, if no BLH exists in the meteorological file, BLH is estimated using the vertical temperature profile. A selection of the BLH-

Helen Langley DeWitt 2/28/15 2:35 PM
Deleted: 4B

Helen Langley DeWitt 2/28/15 2:35 PM
Deleted: 2014).

Helen Langley DeWitt 2/28/15 2:35 PM
Deleted: 4A

scaled diurnal profiles of traffic and biogenic emission related VOC concentrations are shown in Figure 4A along with traffic (speed, vehicular flux) diurnal profiles and the calculated boundary layer heights and measured temperatures (Figure 4B and C). This calculation was performed to more directly compare vehicle concentration and speed to vehicular emissions and temperature with biogenic emissions (by removing the dilution of emissions by the changing boundary layer height). Biogenic species, such as isoprene, peaked in concentration during the afternoon, when temperatures were the warmest. Aromatic species peaked in concentration, even after the rough boundary layer correction was applied, during periods of low speeds. This is consistent with other findings that show cold starts and idling speeds cause an increase in aromatic VOC emissions from gasoline-powered vehicles (e.g., Broderick and Marnane, 2002).

3.3 PMF Analysis

The positive matrix factorization (PMF) model was applied to the HR-ToF-AMS aerosol data using the process described in detail by Ulbrich et al. (2009). Six aerosol factors were resolved by their source and relative aging using the PMF model: a hydrocarbon-like organic aerosol (HOA) factor, a regional oxidized organic aerosol (OOA) factor associated with sulfate aerosol, two oxidized organic aerosol factors with opposing diurnal patterns, one more oxidized than the other (Less Oxidized Organic Aerosol, or LO-OA, with peak concentration during the mornings/nights, and More Oxidized Organic Aerosol, or MO-OA, with peak concentrations during the afternoons), a biomass-burning organic aerosol factor (BBOA), and a nitrogen-containing organic aerosol factor (NOA). The mass spectra for the six resolved factors is shown in Figure 5, labeled with their identifications. Evaluation graphs for the six-factor PMF solution are shown in the Supplementary Information (Figures S5-S8). Polar plots of the factor concentrations and wind direction are shown in Figure S9. A six factor solution was the lowest number of factors where a BBOA factor was resolved; BBOA was suspected to be present in the air mass measured during the campaign due to periods of increased levoglucosan

Helen Langley DeWitt 2/28/15 2:35 PM
Deleted: corrected

Helen Langley DeWitt 2/28/15 2:35 PM
Deleted: 5A

Helen Langley DeWitt 2/28/15 2:35 PM
Deleted: 5B and C).

Helen Langley DeWitt 2/28/15 2:35 PM
Deleted:
3.3

Helen Langley DeWitt 2/28/15 2:37 PM
Deleted: *3.3*

Helen Langley DeWitt 2/28/15 2:35 PM
Deleted:) (Figures 8-10).

Helen Langley DeWitt 2/28/15 2:35 PM
Deleted: 8

Helen Langley DeWitt 2/28/15 2:35 PM
Deleted: S4-S6

Helen Langley DeWitt 2/28/15 2:35 PM
Deleted: S8

511 measured on filter samples. However, its concentrations were very low (15 ng.m^{-3} on average, Polo-
512 Rehn, (2013)) compared to concentrations measured in Grenoble in winter (around 800 ng.m^{-3} (Herich
513 et al., 2014)). Solutions with more than six factors appeared to split the OOA factor further until
514 differences between each OOA factor were difficult to justify. The calculated elemental ratios of O:C,
515 H:C, and Organic Mass: Organic Carbon (OM:OC), (Aiken et al., 2008) are shown in Table 1.
516 The diurnal pattern and the relative concentrations of each resolved factor, averaged over the
517 campaign period, are shown in Figure 6, along with the standard deviation of their concentrations.
518 Morning and evening peaks, correlating in time to rush hour traffic, were clearly observable for the
519 HOA factor. Also clearly visible in Figure 6A is the opposing diurnal trends of LO-OA (peaking at
520 night and early morning) and MO-OA (peaking around 3pm each afternoon). Regional OOA had no
521 discernable diurnal trend. An interesting finding in these data is that the HOA and NOA factor
522 concentrations both peaked during morning and evening high traffic periods (Figure 6A). This is not
523 the general behavior demonstrated in most studies for the NOA factor, although a similar NOA factor
524 has been previously measured in the Po Valley, Italy (Saarikoski et al., 2012). This behavior was
525 confirmed by examining HT periods, with an increase of 1.3x and 1.9x for NOA and HOA
526 concentrations, respectively, during HT periods. While many of larger hydrocarbons or of other
527 organics, only N-containing peaks whose fitting significantly reduced the residual mass at each unit
528 mass were fit (Figure S8). Additionally, and when possible, the w-ToF mode data was examined to
529 determine if the N-containing peak was resolved enough from neighboring peaks for certain
530 identification.
531 In Figure 7, the time series of each factor are shown with oxalate ($C_2O_4^{2-}$, a marker for aged and
532 oxidized organic aerosol), sulfates, and levoglucosan (a marker for biomass burning) measurements
533 from filter samples. Table 2 summarizes the R^2 values between key tracer species and the resolved
534 aerosol factors. The two main factors resolved, in terms of mass concentration, were the OOA factors
535 with opposite diurnal trends, MO-OA and LO-OA. The concentration of MO-OA rose as the aerosol

Helen Langley DeWitt 2/28/15 2:35 PM
Deleted: .

Helen Langley DeWitt 2/28/15 2:35 PM
Moved (insertion) [2]

Helen Langley DeWitt 2/28/15 2:35 PM
Deleted: 9

Helen Langley DeWitt 2/28/15 2:35 PM
Deleted: 9A

Helen Langley DeWitt 2/28/15 2:35 PM
Deleted: 9A

Helen Langley DeWitt 2/28/15 2:35 PM
Deleted: While many

Helen Langley DeWitt 2/28/15 2:35 PM
Deleted: the defined N-containing peaks were adjacent to or in between those

Helen Langley DeWitt 2/28/15 2:35 PM
Deleted: the defined N-containing peaks were adjacent to or in between those

Helen Langley DeWitt 2/28/15 2:35 PM
Deleted: larger hydrocarbons or of

Helen Langley DeWitt 2/28/15 2:35 PM
Deleted: S7

Helen Langley DeWitt 2/28/15 2:35 PM
Deleted: Further discussion of this NOA factor is presented in section 3.4.2.

Helen Langley DeWitt 2/28/15 2:35 PM
Deleted: As suggested by the relative mass contribution of *m/z* 57 and *m/z* 44 (see previous section), HOA was not the largest average contributor to the bulk measured aerosol mass over the campaign period, despite the fact that these measurements were conducted 15 m from a major highway (Figure 9B). The relative size of each type of particle (primary, or HOA, and OOA) likely plays a major role in the relative mass concentrations of each factor. The variability of each factor over the campaign was high as, unlike measurements in more rural areas, the proximity to a primary aerosol source (highway) and to an urban center (Grenoble), as well as large green spaces (the Alps) allowed the full range of aged and locally transported aerosol to be observed at this station. The calculated elemental ratios of O:C, H:C, and N:C, along with the

Helen Langley DeWitt 2/28/15 2:35 PM
Moved up [2]: Organic Mass: Organic Carbon (OM:OC), (Aiken et al., 2008) are shown in Table 1.

Helen Langley DeWitt 2/28/15 2:35 PM
Deleted: The N:C ratios are simply for qualitative reference, as the low signal of N-containing peaks and their high degree of overlap with larger oxygen-containing ... [1]

Helen Langley DeWitt 2/28/15 2:35 PM
Deleted: 10

number-weighted geometric mode diameter rose, also indicative of increasing aerosol age/coagulation. The LO-OA factor resembled the SV-OOA factor reported by Docherty et al. (2008) measured during the Study of Organic Aerosols (SOAR) project at Riverside, CA, which was also found to decrease during the afternoon as temperature and photochemical processing increased. The chemical differences between these two spectra are show in Figure S10 and described in the Supplementary Information. The increase in MO-OA concentration occurred as both PTR-ToF-MS isoprene signal was increasing (also a temperature-related process) and as the 9-carbon aromatic: benzene ($C_9H_{13}^+$:$C_6H_7^+$) VOC ratio was at its minimum (related to photochemical age of air mass, (Parrish et al., 2007) . Thus, the increase MO-OA could be linked to photochemical aging of vehicular emissions during the day and/or to increasing biogenic VOC emissions and their subsequent photochemical aging and condensation into aerosol form.

The BBOA factor was found to correlate with levoglucosan (R^2=0.65, n=38); while significant levels of biomass burning from wood-burning stoves and other combustion-related heating are known to affect the Grenoble Valley in winter, such a large contribution during this season is surprising. Likely the PMF-resolved BBOA factor was somewhat mixed with emissions with close spectral signature (vehicular emissions or potentially cooking aerosol emissions). Episodic local yard-waste burning could also have contributed to the bulk aerosol spectrum, as spikes in the BBOA concentration do not appear to correlate with a particular wind direction (Figure S9). The ratio of levoglucosan: BBOA is quite low (0.03); however, it is within the order of magnitude of previously reported measurements (e.g., 0.06, (Aiken et al., 2009)). Additionally, the higher levels of oxidants found in the atmosphere in the summer could cause a faster degradation of levoglucosan in the atmosphere after emission (Hennigan et al., 2010). Thus, the BBOA concentrations reported here shall be considered as an upper limit of the biomass burning contribution.

Of the factors resolved, the HOA factor had the lowest O: C ratio (0.07) and a good (R^2=0.58, n=3928) correlation with BC concentration. The mass spectrum of the resolved HOA factor highly

Helen Langley DeWitt 2/28/15 2:35 PM
Moved (insertion) [3]

Helen Langley DeWitt 2/28/15 2:35 PM
Deleted:) ;

Helen Langley DeWitt 2/28/15 2:35 PM
Deleted:), although the separation of further factors did not appear to separate cooking and biomass burning influences within the measured bulk aerosol.

Helen Langley DeWitt 2/28/15 2:35 PM
Deleted: S8

Helen Langley DeWitt 2/28/15 2:35 PM
Deleted: .

Helen Langley DeWitt 2/28/15 2:35 PM
Deleted: Oxalate and regional OOA covaried with an R^2 of 0.62 (n=53). Regional OOA was identified as thus due to its low temporal variation, its correlation with SO_4, and a low correlation with wind direction (Figure S8). This factor was removed from the atmosphere during periods of rain and experienced a slow recovery afterwards. At the beginning of the experiment (Sept 11th-13th), regional OOA and SO_4 did not correspond; however, during the middle and end of the campaign, temporal variations of the regional OOA and SO_4 corresponded fairly well (R^2=0.65, n= 3328). The reason for the initial high SO_4 and low regional OOA is unclear from the data set as-is; however, MO-OA and SO_4 also had similar time series trends (R^2=0.50, n=3328) and MO-OA was high at the beginning of the campaign. The closeness of the two spectra's composition, as well as the nature of the aerosol type (not from a specific source but rather aged bulk organic aerosol), in which variations would logically occur, may have led to the imprecise separation of these two factor types.

Helen Langley DeWitt 2/28/15 2:35 PM
Deleted: , which suggests it was primary and from vehicular origin.

resembled (R^2>0.95, n=100) previously resolved HOA factors and direct AMS measurements of diesel and gasoline emissions (Mohr et al., 2009; Zhang et al., 2005). HOA was not the largest average contributor to the bulk measured aerosol mass over the campaign period, despite the fact that these measurements were conducted 15 m from a major highway. The relative size of each type of particle (primary, or HOA, and OOA) likely played a major role in the relative mass concentrations of each factor (Figure S11 and discussion), and the higher increase above background of particle number versus particle mass found in this study agrees with previous studies (Karner et al., 2010, Sun et al., 2010). The variability of each factor over the campaign was high as, unlike measurements in more rural areas, the proximity to a primary aerosol source (highway) and to an urban center (Grenoble), as well as large green spaces (the Alps) allowed the full range of aged and locally transported aerosol to be observed at this station.

3.3.1 Fossil and Modern Carbon

A source of uncertainty in the global particulate emissions of vehicles is the formation of SOA from gas-phase emissions and the aging of POA. To discriminate between the relative concentration of modern and fossil carbon, and thus potentially discriminate between OOA from vehicular sources and from modern sources, daily filter samples were collected at the sampling site and 14C radiocarbon measurements were performed. From these measurements, the percentage of modern carbon from TC (OC+EC) was calculated. Modern carbon varied from 15-36% of the total aerosol carbon, a significant portion of the measured carbon considering the close proximity of the measurements to fossil carbon sources. In France, the contribution of biofuel was about 7% and 5% for diesel and gasoline fuel, respectively, in 2011 (UFIP, Union Française des Industries Petrolières, 2011) and cannot explain this relative high proportion of modern carbon observed in the particulate matter. This is similar to findings shown in Hodzic et al. (2010), Minguillon et al. (2011), and El Haddad et al. (2013), which indicate that modern carbon is often more significant than fossil carbon in the carbonaceous fraction of PM, even in cities with high vehicular emissions (e.g., Mexico City, Barcelona or Marseille).

Helen Langley DeWitt 2/28/15 2:35 PM
Deleted: . ... [2]

Helen Langley DeWitt 2/28/15 2:35 PM
Deleted: , were the OOA factors with opposite diurnal trends, MO-OA and LO-OA. The concentration of MO-OA rose as the aerosol number-weighted geometric mode diameter rose, also indicative of increasing aerosol age/coagulation. The LO-OA factor resembled the SV-OOA factor reported by Docherty et al. (2008) measured during the Study of Organic Aerosols (SOAR) project at Riverside, CA, which was also found to decrease during the afternoon as temperature and photochemical processing increased. Figure 11 shows the normalized difference between HOA and LO-OA (panel a) and LO-OA and MO-OA (panel b). A relative reduction in the higher-mass hydrocarbon fragments and an increase in the oxidized organic fragments are observed between HOA and LO-OA. This difference spectrum is similar to that found by Sun et al., (2012) between spectra obtained just prior to and during peaks in traffic (when the spectra would be mostly comprised of HOA). The main difference between LO-OA and MO-OA was the level of oxidation; the *m/z* 44 and 28 (COO^+ and CO^+, respectively) increased in MO-OA while the rest of fragments decreased in relative concentration. The increase in MO-OA concentration occurred as both PTR

Helen Langley DeWitt 2/28/15 2:35 PM
Moved up [3]: -MS isoprene signal was increasing (also a temperature-related process) and as the 9-carbon aromatic: benzene ($C_9H_{13}^+$:$C_6H_7^+$) VOC ratio was at its minimum (related to photochemical age of air mass, (Parrish et al., 2007) .

Helen Langley DeWitt 2/28/15 2:35 PM
Deleted: Thus, the increase MO-OA could be linked to photochemical aging of vehicular emissions during the day and also to increasing biogenic VOC emissions and their subsequent photochemical aging and condensation into aerosol form.

Helen Langley DeWitt 2/28/15 2:35 PM
Moved (insertion) [4]

Helen Langley DeWitt 2/28/15 2:35 PM
Moved (insertion) [5]

As radiocarbon measurements have been performed through a thermal approach (combustion of the samples at 850°C), we consider in the following section EC measured by the thermo-optical method. As shown in figure S12, EC and BC do not agree well at low mass loadings, but have a wider scatter in the data at higher mass loadings. The calculation of BC (measured by the MAAP) using an absorption cross-section is imprecise and, at high loadings of BC, may under or overestimate this mass loading. Figure S12 shows a comparison between the MAAP (BC) and thermal measurement (EC) data, with a 1:1 line. As the thermal-optical analysis of EC is a more direct analysis, EC was chosen to be used in this calculation.

Assuming that the majority of EC was traffic-related, and thus from fossil origin, the concentration of modern organic carbon and fossil organic carbon was then calculated. While evidence for the presence of biomass burning aerosol was measured at the field site, the main source of EC was likely diesel exhaust. Figure 8 shows the fraction of EC and OC, HOA, and a partitioning between fossil and modern carbon. In Figure 8A, a rough calculation was performed to determine the concentration of non-primary fossil organic carbon. For a first estimate, all EC was assumed to be fossil in origin. Additionally, the HOA aerosol was also assumed to be vehicular, and thus fossil, in origin. The HOA factor concentration has been divided by its OM: OC ratio to remove any non-carbon mass (HOA C, calculated from the elemental formulas of the PMF factor mass spectra, Aiken et al. (2008)). Both EC and HOA C had high (R^2=0.89 and 0.85 respectively, n=10) correlations with the fossil C mass, which supported a largely fossil source for these two species. The remaining fossil organic carbon mass after subtraction was then assumed to be from non-primary sources (in light blue).

This calculation provided a lower estimate of the amount of fossil carbon contributing to SOA mass, and involves several assumptions and potential sources of error. Sources of error in this calculation include error in the PMF resolution of primary (HOA) organic aerosol spectra and error in the calculated OM:OC ratio of this factor species, biodiesel vehicular emissions contributing modern

carbon to measured HOA, and biomass burning aerosol contributing modern carbon to measured EC. As the measured HOA:EC ratio was in-line with previous measurements in high diesel environments, HOA concentrations did not appear to be significantly over or under estimated. Up to 7% of fuel use in France was biodiesel, thus, part of the HOA concentration could be from modern sources. While research has shown that the use of biodiesel fuels reduces the overall primary particulate matter emissions (Cheung et al, 2010), biodiesel could still be a modern carbon contributor to OC and EC mass. Additionally, although the concentration of BBOA was generally low (a campaign average of 0.34 ± 0.23 μg m^{-3}) and the ratio of BBOA:EC has been found to be on the order of 3-4 in other areas of France (Crippa et al., 2013), some contribution to EC from biomass burning may have been present at the measurement site. In Figure 8B, a range of fossil non-primary organic carbon, normalized to total measured organic carbon, is presented. For the upper limit of this range, HOA C and EC were considered to be 95% fossil and 5% modern (7% biodiesel fuel use and an estimated 25% reduction in particulate emissions from biodiesel fuel). Also for this upper limit, the calculated concentration of BBOA was divided by 3 and used to calculate possible modern EC from biomass burning (Crippa et al., 2013).

Helen Langley DeWitt 2/28/15 2:35 PM
Moved (insertion) [6]

Helen Langley DeWitt 2/28/15 2:35 PM
Moved (insertion) [7]

Total organic carbon concentration appeared to be more driven by processed/aged OOA concentrations than by primary emissions. During the period with the highest organic concentrations (September 15th-17th), most of the non-HOA carbon measured was modern carbon. Also during this time period, the winds were also slightly more southerly and SO_4 and OOA concentrations increased, which could indicate a more regional contribution to the measured air mass during this time. After a period of heavy rain on the 19th, almost none of the non-HOA, organic carbon was fossil; however, this also coincided with a period of increased BBOA, which may have contributed to modern-EC emissions and thus an underestimate of fossil-OC emissions (Figure 7). At other times during the campaign, HOA concentrations alone could not adequately explain all of the measured fossil organic carbon and additional sources of fossil organic carbon (such as photochemical reactions forming aerosol from

Helen Langley DeWitt 2/28/15 2:35 PM
Moved (insertion) [8]

vehicular VOC emissions) would be needed. Additionally, the origin of the NOA factor remains unclear, and if fossil in origin, could explain part of the non-HOA organic fossil carbon measured at the site, further reducing the OOA fossil-C (at times to almost zero). Overall, throughout the campaign the majority of OOA observed was most probably modern in origin.

The high levels of modern carbon OOA suggested that biogenic compounds had a large effect on the overall aerosol population in this location, even directly adjacent to a large anthropogenic emission source (i.e., traffic). Interaction between anthropogenic oxidants and biogenic VOCs (or BVOCs) has been found to increase the formation of SOA (Chameides et al., 1988; Goldstein et al., 2009; Shilling et al., 2013), isoprene oxidation reactions leading towards SOA have been shown to vary depending on the level of NOx (Chen et al., 2014; Kroll et al., 2005; Ng et al., 2007; Xu et al., 2014), and likely BVOC concentrations were greater and the aromatic VOC concentrations were lower in the wider Grenoble Valley.

3.4.3. Differences between diesel-heavy and gasoline-heavy near-roadway measurements

Older diesel vehicles have been shown to emit both higher levels of PM, particularly BC, and higher levels of NOx. Indeed, high concentrations of NOx were measured at the field site, up to 450 ppbv ($NO+NO_2$), for 15 min averaged measurements. NO_2 levels exceeded the 100 ppbv European hourly limit almost every morning. The campaign average for NO_2 was 94 +/- 64 ppbv. For comparison, at a measurement site adjacent to a major highway in New York, Sun et al. (2012) measured an average of 48 +/- 30 ppbv NO_2, about half that of this campaign's average, with 15 min average peaks ranging from 100-300 ppbv. The hourly traffic concentrations at each site were close (approximately 10,000 vehicles/hour reported during the Sun et al. (2012) measurement periods compared to approximately 8,000 vehicles/hour observed during daylight driving hours on Grenoble's highway); thus, increased NOx cannot be explained by increased traffic. Rather, increased diesel fuel use is a very likely hypothesis.

High levels of BC were also measured in this work. A comparison of the HOA: BC ratio from

Helen Langley DeWitt 2/28/15 2:35 PM
Deleted: The PMF model was also run with unit-mass resolution (UMR) AMS data. In such a configuration, all HR factors except the NOA factor were resolved; however, the concentration of HOA rose as other species (oxidized organic peaks that share nominal masses with hydrocarbons; N-containing peaks) were folded into the HOA factor ... [3]

Helen Langley DeWitt 2/28/15 2:35 PM
Deleted: To better compare our HOA factor concentration and BC concentration with previously published studies, the UMR HOA factor concentration was used

Helen Langley DeWitt 2/28/15 2:35 PM
Deleted: calculate the concentration

Helen Langley DeWitt 2/28/15 2:35 PM
Deleted: HOA

Helen Langley DeWitt 2/28/15 2:35 PM
Deleted: a ratio

Helen Langley DeWitt 2/28/15 2:35 PM
Moved (insertion) [9]

Helen Langley DeWitt 2/28/15 2:35 PM
Deleted: ~0.26 HOA:BC was found (~0.19

Helen Langley DeWitt 2/28/15 2:35 PM
Deleted: HR HOA:BC). The

Helen Langley DeWitt 2/28/15 2:35 PM
Moved (insertion) [10]

Helen Langley DeWitt 2/28/15 2:35 PM
Moved (insertion) [11]

Helen Langley DeWitt 2/28/15 2:35 PM
Moved (insertion) [12]

this study and from previously reported field studies is shown in Figure 9A. As expected, since the French fleet includes a much higher percentage of diesel car with increased BC emissions, this ratio was significantly lower than that reported for an urban-downwind site in Pittsburgh (1.41, Zhang et al. (2005)), a highway adjacent site in New York (1.02, Sun et al. (2012)), an urban/highway site in Ontario (0.7-1.1, Stroud et al. (2012)), a rural site in NW England (1.61-1.91, Liu et al. (2006)), and an urban site in Zürich, Switzerland (1.1, Lanz et al. (2007)). As for measurements in France, a study in an urban site in Paris observed a HOA:BC ratio of 0.61 (Crippa et al., 2013); this site was most probably influenced by a vehicle fleet similar to Grenoble's, but measurements were collected during winter (lower temperatures) and within Paris (increased urban emissions). Tailpipe measurements of Euro 4 diesel and gasoline-powered vehicles (a Renault Kangoo and a Ford Ka, respectively) at IFSTTAR (Institut Français des Sciences et Technologies des Transports, de l'Aménagement et des Réseaux) performed during this PM Drive research program also show a much higher HOA: BC ratio for gasoline vehicles versus diesel vehicles (unpublished data). This was due to much higher BC emissions from the diesel vehicle, as opposed to higher HOA emissions from the gasoline vehicle. Similarly, the HOA factor measured near Grenoble was similar to that measured by Sun et al. (2012), in a high gasoline environment next to a highway in New York, both in absolute concentration and chemical composition; thus, an increase in BC emissions (from diesel) rather than a reduction in HOA: vehicle number was likely the cause of our low HOA: BC ratio.

The change in HOA: BC ratio as a function of the diesel: gasoline fuel use (Road sector, World Bank, 2011) is shown in Figure 9B. A decrease in HOA: BC with an increase in percent diesel is clearly observable with a strong correlation (R^2=0.85, n=10), despite the many different factors possibly influencing BC and HOA concentrations at each location (e.g., local aerosol sources, meteorology). Such a linear relationship between HOA: BC and diesel percentage is very interesting, but was not necessarily expected, since the emission factors of HOA+BC differ significantly between diesel and gasoline cars, especially for pre EURO5 vehicles.

Helen Langley DeWitt 2/28/15 2:35 PM
Deleted: 12

Helen Langley DeWitt 2/28/15 2:35 PM
Deleted:)

Helen Langley DeWitt 2/28/15 2:35 PM
Deleted: Zurich

Helen Langley DeWitt 2/28/15 2:35 PM
Deleted: This low HOA:BC ratio in the campaign in Grenoble is in-line with reported measurements from diesel exhaust; for example, Chirico et al. (2010) found a OA:BC ratio of 0.28 in smog chamber emission (where most of the OA is likely to be 'HOA-type' aerosol).

Helen Langley DeWitt 2/28/15 2:35 PM
Formatted: Indent: First line: 0"

Helen Langley DeWitt 2/28/15 2:35 PM
Deleted: The

Helen Langley DeWitt 2/28/15 2:35 PM
Moved up [11]: The hourly traffic concentrations at each site were close (approximately 10,000 vehicles/hour reported during the Sun et al.

Helen Langley DeWitt 2/28/15 2:35 PM
Deleted: .

Helen Langley DeWitt 2/28/15 2:35 PM
Deleted: (2012) measurement periods compared to approximately 8,000 vehicles/hour observed during daylight driving hours in the Grenoble's highway);

Helen Langley DeWitt 2/28/15 2:35 PM
Deleted: Although HDV have higher PM emission limits than LDVs for the same Euro classification, the HOA: BC ratio remained fairly steady throughout the day even as the LDV: bus/HDV ratio increased by a factor of four from morning to evening. This suggested that LDVs, rather than HDVs or buses, were more responsible for the low HOA: BC ratio and the high BC concentrations. This differs from the Sun et al. (2012) measurements. Sun et al. (2012) attribute a period of strong correlation between BC and HOA, along with a low HOA: BC ratio (of 1.02) to the influence of diesel trucks (12%) and a day of high HOA with little to no BC due to the influence of local bus emissions powered by compressed natural gas.

Helen Langley DeWitt 2/28/15 2:35 PM
Deleted: Of the measurements presented in Figure 12, the French measurement sites had by far the highest proportion of diesel vehicles and diesel fuel use.

Helen Langley DeWitt 2/28/15 2:35 PM
Deleted: 13

Additionally, an AMS factor with a diurnal pattern peaking during rush hour and with N-containing peaks was observed. Saarikoski et al., (2012) found a similar amine-containing NOA factor in measurements taken in the Po Valley (Italy) that also had a strong diurnal pattern. However, their NOA factor was attributed to marine influence due to a correlation with MSA (Saarikoski et al., 2012), although it is possible that MSA was from the local industrial use of DMSO as a solvent, and had a higher H:C ratio (1.91) than the factor resolved from this data set (1.38). Like France, Italy has a large percentage of diesel fuel consumption (71%, World Bank 2011). Aiken et al., (2009) and Sun et al., (2011) also resolved N-containing OA factors from data measured in Mexico City and New York, respectively, but did not observe a similar diurnal pattern. In the PTR-ToF-MS mass spectra results obtained from Euro 5 vehicle emission smog chamber studies, Hellebust et al., (2015 and 2013) found higher nitrogen-containing emissions from fresh and aged diesel mass than from fresh and aged gasoline mass spectra (e.g., peaks such as $CH_4NO_2^+$). Similar nitrogen-containing VOC peaks were found by Inomata et al. (2013) in diesel exhaust. Thus, diesel-related emissions could possibly be the source for the observed NOA factor, although no significant correlation between this factor and other vehicular emissions, such as BC, was found. More detail on the NOA factor can be found in the Supplementary Information and Figure S13.

And finally, only small amounts OOA measured at the field site were calculated to contain fossil-OC. Work by Bahreini et al., (2010) found that much of the measured SOA in the Los Angeles Valley was from gasoline passenger cars, not from diesel trucks, and perhaps the relatively low concentration of gasoline vehicles on the road in France is related to the low concentration of fossil-OOA.

4. Conclusions

During this campaign, highly time resolved particle and gas-phase chemical composition and

Helen Langley DeWitt 2/28/15 2:35 PM
Moved up [9]: NO_2 levels exceeded the 100 ppbv European hourly limit almost every morning. The campaign average for NO_2 was 94 +/- 64 ppbv.

Helen Langley DeWitt 2/28/15 2:35 PM
Deleted: *3.4.2. NO/NOx/Nitrogen* ... [4]

Helen Langley DeWitt 2/28/15 2:35 PM
Deleted: For comparison, Sun et al.

Helen Langley DeWitt 2/28/15 2:35 PM
Moved up [10]: (2012) measured an average of 48 +/- 30 ppbv NO_2, about half that of this campaign's average, with 15 min average peaks ranging from 100-300 ppbv.

Helen Langley DeWitt 2/28/15 2:35 PM
Formatted: Indent: First line: 0.49"

Helen Langley DeWitt 2/28/15 2:35 PM
Deleted: Since, as mentioned earlier vehicle fluxes were similar at both sites, … diff ... [5]

Helen Langley DeWitt 2/28/15 2:35 PM
Moved up [12]: . Rather, increased diesel fuel use is a very likely hypothesis.

Helen Langley DeWitt 2/28/15 2:35 PM
Deleted: One possible effect of increased NOx on aerosol formation is the formation of organic nitrate aerosols from the photochemical reactions of various VOC precursors in the presence of high levels of NOx (Ng et al., 2007). During the field campaign, little evidence of typical organic nitrate peaks (e.g., CH_4NO, C_2H_5NO, C_3H_4NO, CH_2NO_3, CH_2NO_2 (Farmer et al., 2010) was found in the high resolution mass spectra. In low concentrations, organic ... [6]

Helen Langley DeWitt 2/28/15 2:35 PM
Moved up [4]: Modern carbon varied from 15-36% of the total aerosol carbon, a ... [7]

Helen Langley DeWitt 2/28/15 2:35 PM
Deleted: In France, the contribution of biofuel were about 7% and 5% for diese ... [8]

Helen Langley DeWitt 2/28/15 2:35 PM
Moved up [5]: , respectively, in 2011 (UFIP, Union Française des Industries Petrolière ... [9]

Helen Langley DeWitt 2/28/15 2:35 PM
Deleted: (e.g., Mexico City, Barcelona or Marseille).

Helen Langley DeWitt 2/28/15 2:35 PM
Formatted: Indent: First line: 0.49"

Helen Langley DeWitt 2/28/15 2:35 PM
Deleted: Assuming that the majority of BC was traffic-related, and thus from f ... [10]

Helen Langley DeWitt 2/28/15 2:35 PM
Moved up [6]: has been found to be on the order of 3-4 in other areas of France (C ... [11]

Helen Langley DeWitt 2/28/15 2:35 PM
Deleted: Overall, throughout the campaign the majority of SOA observed was mo ... [12]

concentration measurements were obtained alongside parallel traffic data of the speed, fluxes, vehicle type, and fuel type of passing cars on a highway in the Grenoble Valley. An analysis of the local primary (traffic) aerosol and the more regional, aged secondary organic aerosol was performed for the PM1 fraction observed by the HR-ToF-AMS. The PMF model was run on the high-resolution HR-ToF-AMS aerosol data and six factors were resolved from the bulk aerosol data: 1) an HOA factor, related to traffic 2) a BBOA factor 3) a regional OOA factor, which covaried with sulfate 4) a MO-OA factor, increasing in concentration during sunny afternoons 5) a LO-OA factor, with the opposite diurnal pattern as MO-OA, likely due to gas-particle phase partitioning and photochemical processing and 6) an NOA factor with a diurnal pattern similar to that of HOA and to traffic peaks.

The resolved mass spectrum for the HOA factor was chemically similar to mass spectra from both gasoline and diesel-emitted organic carbon and previously resolved HOA factors in high-gasoline environments; however, the HOA: BC ratio measured was low (<0.3) throughout the campaign. This ratio agrees with previously reported HOA: BC ratios in high diesel environments and from direct measurements of diesel emissions in smog chamber and tailpipe measurement studies. The fraction of diesel-powered vehicles on the road appeared to control, to some extent, this ratio. Diesel also influenced local NOx concentrations, as the measured NOx was two times higher than concentrations near a similarly-trafficked highway in New York, USA.

While high levels of both black carbon (5 +/- 3 μg m^{-3}) and organic aerosol (8 +/- 4 μg m^{-3}) were measured, when examined, only 20% of the total organic mass signal could be attributed to primary vehicular emissions (i.e., HOA). Significant amounts of modern organic carbon were also measured, and fossil carbon appeared to contribute only a small amount to the measured OOA. Although NOx and VOCs emitted by diesel and gasoline engines, respectively, may have influenced SOA formation in the Grenoble Valley, the majority of OOA measured was modern in origin, even adjacent to a major source of fossil carbon. Whether this is due to a lower overall gas+particle emission of diesel vehicles, the lack of aromatic compounds in diesel VOC emissions, high NOx

Helen Langley DeWitt 2/28/15 2:35 PM
Deleted: A complete

Helen Langley DeWitt 2/28/15 2:35 PM
Deleted: Periods of heavy traffic were associated with both increased HOA and BC along with increased particle number concentration and lower particle size.

Helen Langley DeWitt 2/28/15 2:35 PM
Deleted: HOA). Traffic emissions dominated the aerosol particle number concentration, but the majority of the organic aerosol mass concentration measured was SOA. NOx concentrations in these measurements were two times higher than concentrations near a similarly-trafficked highway in New York, USA.

Helen Langley DeWitt 2/28/15 2:35 PM
Deleted: SOA

reducing the efficiency of vehicular VOC to SOA formation mechanisms, an acceleration of BVOC to biogenic aerosol formation in the presence of vehicular emissions, or simply the more global source and higher efficiency of BVOC to SOA reactions is unclear, but in a high diesel environment, SOA OOA from fossil-fuel carbon was only a small source of the measured OOA , while modern C-containing OOA dominated the organic aerosol mass in the fine fraction of PM1.

Helen Langley DeWitt 2/28/15 2:35 PM
Deleted: carbonaceous

Helen Langley DeWitt 2/28/15 2:35 PM
Deleted:

Helen Langley DeWitt 2/28/15 2:35 PM
Formatted: Indent: First line: 0"

Acknowledgments:

This work was supported by the French Environment and Energy Management Agency (ADEME, Grant number 1162C0002). The authors gratefully acknowledge the NOAA Air Resources Laboratory (ARL) for the provision of the HYSPLIT transport and dispersion model (http://www.ready.noaa.gov) used in this publication. We also gratefully acknowledge Air Rhone Alpes staff (particularly Yann Pellan) for their support during the campaign as well as Y. Sun and Q. Zhang for providing near-highway aerosol data from their paper Sun et al., (2012) for comparison with these measurement, and the MASSALYA instrumental platform (Aix Marseille Université, lce.univ-amu.fr) for the analysis and measurements used in this publication. Finally, the authors would like to acknowledge and thank the two anonymous reviewers who provided constructive advice on the formation of the final paper.

Helen Langley DeWitt 2/28/15 2:35 PM
Deleted: *1162C00O2). Traffic data was analyzed by Anaïs Pasquier (LTE IFSTTAR) and Michel André.*

Helen Langley DeWitt 2/28/15 2:35 PM
Deleted: *measurements.*

Helen Langley DeWitt 2/28/15 2:35 PM
Deleted: *Finally, the authors gratefully acknowledge*

1261

Table 1

PMF FACTOR	OM:OC	H:C	O:C
HOA	1.25	1.89	0.07
NOA	1.69	1.38	0.4
LO-OA	1.74	1.34	0.47
MO-OA	2.15	1.16	0.78
BBOA	1.56	1.47	0.32
OOA-REG	1.85	1.54	0.52

Helen Langley DeWitt 2/28/15 2:35 PM
Deleted: N:C[1]

Helen Langley DeWitt 2/28/15 2:35 PM
Deleted Cells

Helen Langley DeWitt 2/28/15 2:35 PM
Formatted Table

Helen Langley DeWitt 2/28/15 2:35 PM
Deleted: 0.002

Helen Langley DeWitt 2/28/15 2:35 PM
Deleted: 0.028

Helen Langley DeWitt 2/28/15 2:35 PM
Deleted: 0.005

Helen Langley DeWitt 2/28/15 2:35 PM
Deleted: 0.001

Helen Langley DeWitt 2/28/15 2:35 PM
Deleted: 0.01

Helen Langley DeWitt 2/28/15 2:35 PM
Deleted: 0.0006

Helen Langley DeWitt 2/28/15 2:35 PM
Deleted: [1] N:C ratio is not quantitative and is only shown to illustrate potential presence of nitrogen-containing organic aerosol in each factor.

PMF FACTOR	Oxalate (N=53) R^2	BC[a] (N=3928) R^2	Levoglucosan (N=38) R^2	Sulfate (N=3328)[b] R^2
HOA	0.01	0.58	0.12	0.004
BBOA	0.04	0.05	0.65	0.005
MO-OA	0.50	0.01	0.02	0.54
LO-OA	0.32	0.01	0.08	0.07
NOA	0.01	0.09	0.12	0.06
OOA-REG	0.62	0.02	0.01	0.65

[a.] BC data smoothed to remove underestimated BC concentrations during periods of high filter loading (Hyvärinen et al., 2013)

[b.] R^2 value calculated after initial high SO_4 period.

Figure Captions

Figure 1: The measurement site location is marked by a red square on the map, and the adjacent highway has been colored in red. A detailed view of the measurement site and the two measurement stations is shown in the lower right-hand corner in the upper right-hand corner is the wind rose and polar plots for black carbon and NO, with the red lines denoting the direction of the highway. Grenoble is to the north.

Figure 2: The non-refractory submicrometer aerosol concentration in μg m^{-3} of SO_4, NH_4, NO_3, and Organic species is plotted along with black carbon both for the campaign time series and the average concentration of each species for the whole campaign and during high traffic periods (A), 15 minute traffic concentration (missing data due to malfunction in the traffic cameras on those days) (B) COO^+ (*m/z* 44) and $C_4H_9^+$ (*m/z* 57) (C), and the number-weighted geometric size distribution (D) with the total number concentration of particles as a function of time (D, right axis).

Figure 3: The concentration in ppbv of PTR-ToF-MS VOC species identified isoprene and MVK/Methacrolin (left axis, A), VOC species associated with diesel exhaust ($CH_4NO_2^+$, $C_2H_5O^+$, B),VOC species associated with gasoline exhaust ($C_6H_7^+$, C_9H13^+, C). NO and NO_2 (gas-phase) ppbv concentrations (D) and ambient temperature (right axis, A) during the measurement period are also shown.

Figure 4: Diurnal profiles of boundary-layer scaled VOC peaks from PTR-ToF-MS measurements and BC peaks from MAAP measurements (A), temperature (right axis, B), boundary layer height (left axis, B), vehicular speed (left axis, C) and vehicle concentration (right axis, C).

Figure 5: The mass spectra of the six resolved factors, more oxidized organic aerosol (MO-OA), less oxidized organic aerosol (LO-OA), regional oxidized organic aerosol (reg-OOA), biomass burning organic aerosol (BBOA), hydrocarbon-like organic aerosol (HOA), and nitrogen-containing organic aerosol (NOA). Fraction of total signal is plotted against *m/z* and the peaks are color-coded to show their high-resolution identifications.

Figure 6: The diurnal profiles (A) and concentration and standard deviation of the six resolved aerosol factors (B).

Figure 7: The time series of the six-factor PMF solution (A), the resolved BBOA factor time series concentration (right axis, B) and off-line levoglucosan measurements (left axis, B), the resolved HOA factor time series concentration and BC (right axis, C), HR-TOF-AMS-measured SO_4 and the resolved regional OOA factor (left axis, D) and off-line oxalate measurements (right axis, right). The inset shows the calculated mass contribution during all (left) and high traffic (right) periods of each resolved PMF factor.

Figure 8:
Calculated HOA and measured BC concentrations from the campaign and HOA: BC ratios from previous field campaigns. Grey area is shaded to include a diesel-only environment and two French HOA: BC ratios: one from Crippa et al., (2013) and from this study (A). The HOA: BC ratio from various literature sources versus percent diesel fuel use out of total fuel use for the country of study

Helen Langley DeWitt 2/28/15 2:35 PM
Deleted:

Helen Langley DeWitt 2/28/15 2:35 PM
Deleted: ... [13]

Helen Langley DeWitt 2/28/15 2:35 PM
Deleted: ... [14]

Helen Langley DeWitt 2/28/15 2:35 PM
Formatted ... [15]

Helen Langley DeWitt 2/28/15 2:35 PM
Deleted: Figure 2 ... [16]

Helen Langley DeWitt 2/28/15 2:35 PM
Deleted: 3… The non-refractory ... [17]

Helen Langley DeWitt 2/28/15 2:35 PM
Deleted: ... [18]

Helen Langley DeWitt 2/28/15 2:35 PM
Formatted ... [19]

Helen Langley DeWitt 2/28/15 2:35 PM
Deleted: 4

Helen Langley DeWitt 2/28/15 2:35 PM
Deleted: Page Break ... [20]

Helen Langley DeWitt 2/28/15 2:35 PM
Formatted ... [21]

Helen Langley DeWitt 2/28/15 2:35 PM
Formatted ... [22]

Helen Langley DeWitt 2/28/15 2:35 PM
Deleted: 5… Diurnal profiles of bou ... [23]

Helen Langley DeWitt 2/28/15 2:35 PM
Formatted ... [24]

Helen Langley DeWitt 2/28/15 2:35 PM
Moved down [13]:

Helen Langley DeWitt 2/28/15 2:35 PM
Deleted: 6: Diurnally averaged BC ... [26]

Helen Langley DeWitt 2/28/15 2:35 PM
Moved down [14]:

Helen Langley DeWitt 2/28/15 2:35 PM
Deleted: 7: The SO_4, NH_4, NO_3, and ... [27]

Helen Langley DeWitt 2/28/15 2:35 PM
Moved down [15]:

Helen Langley DeWitt 2/28/15 2:35 PM
Deleted: ... [25]

Helen Langley DeWitt 2/28/15 2:35 PM
Deleted: 8… The mass spectra of th ... [28]

Helen Langley DeWitt 2/28/15 2:35 PM
Formatted ... [29]

Helen Langley DeWitt 2/28/15 2:35 PM
Deleted: 9

Helen Langley DeWitt 2/28/15 2:35 PM
Deleted: Page Break ... [30]

Helen Langley DeWitt 2/28/15 2:35 PM
Deleted: Page Break ... [31]

Helen Langley DeWitt 2/28/15 2:35 PM
Formatted ... [32]

Helen Langley DeWitt 2/28/15 2:35 PM
Moved (insertion) [13] ... [33]

Helen Langley DeWitt 2/28/15 2:35 PM
Formatted ... [34]

(B).

Figure 9: Measured EC and OC, with calculated contribution of non-primary fossil organic carbon (assuming 100% fossil EC and HOA, A) and assuming partial modern organic carbon EC and HOA contribution (B). The possible fossil OOA (light blue) was calculated by the subtraction of HOA from the fossil-OC fraction (assuming HOA either all fossil, A, or 95% fossil, B, and EC either all fossil (a) or 5%+BBOA/3 modern (b).

Helen Langley DeWitt 2/28/15 2:35 PM
Moved (insertion) [14]

Helen Langley DeWitt 2/28/15 2:35 PM
Formatted: Tabs: 2.14", Left + Not at 3.08"

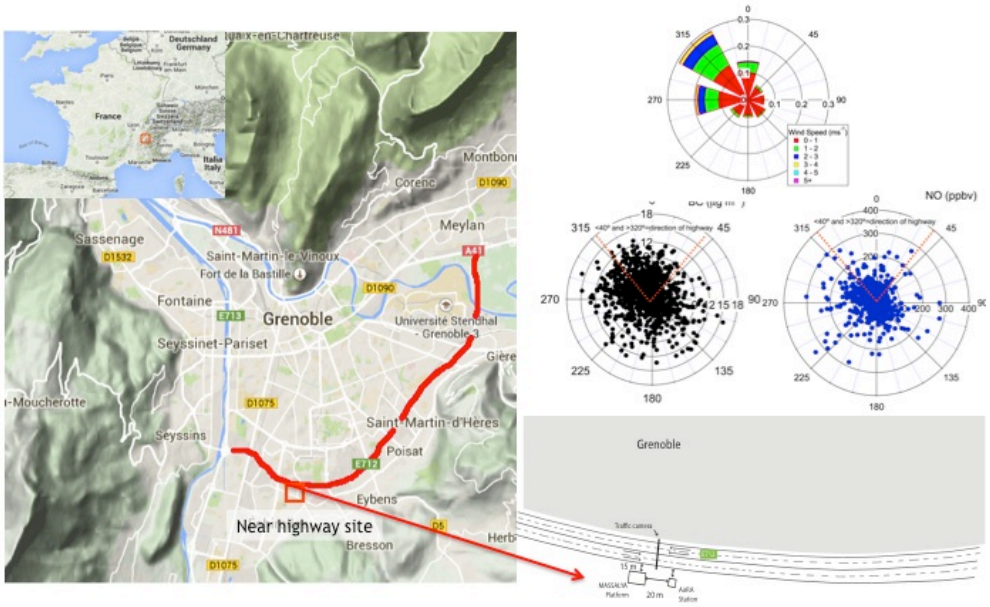

Figure 1
The measurement site location is marked by a red square on the map, and the adjacent highway has been colored in red. A detailed view of the measurement site and the two measurement stations is shown in the lower right-hand corner in the upper right-hand corner is the wind rose and polar plots for black carbon and NO, with the red lines denoting the direction of the highway. Grenoble is to the north.

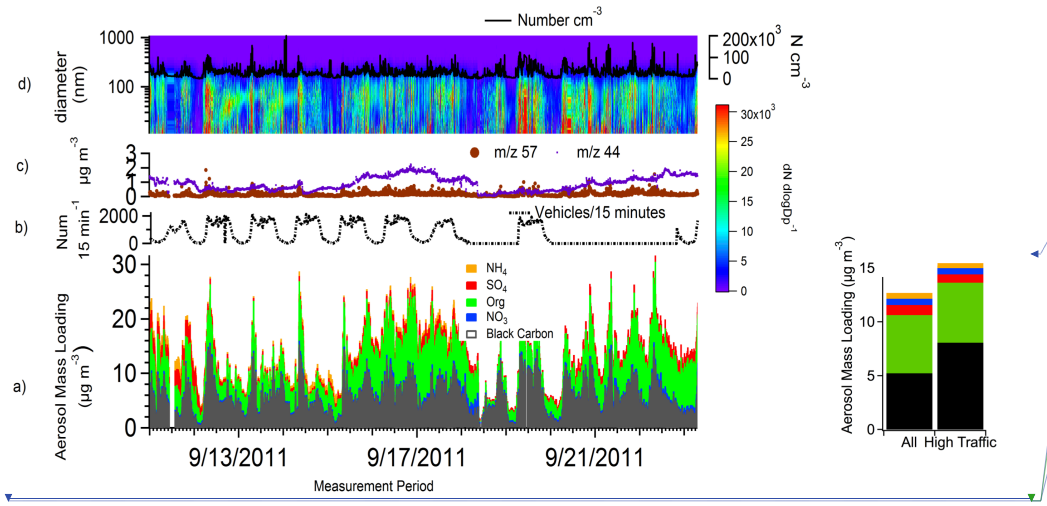

Figure 2: The non-refractory submicrometer aerosol concentration in μg m^{-3} of SO_4, NH_4, NO_3, and Organic species is plotted along with black carbon both for the campaign time series and the average concentration of each species for the whole campaign and during high traffic periods (A), 15 minute traffic concentration (missing data due to malfunction in the traffic cameras on those days) (B) COO^+ (*m/z* 44) and $C_4H_9^+$ (*m/z* 57) (C), and the number-weighted geometric size distribution (D) with the total number concentration of particles as a function of time (D, right axis).

Helen Langley DeWitt 2/27/15 8:01 PM
Deleted: <*sp*>

Helen Langley DeWitt 2/28/15 2:35 PM
Moved (insertion) [15]

Helen Langley DeWitt 2/28/15 2:35 PM
Formatted: No widow/orphan control, Don't hyphenate, Don't adjust space between Asian text and numbers, Font Alignment: Baseline, Tabs: 3.08", Left

Helen Langley DeWitt 2/28/15 2:35 PM
Deleted: 11: Difference

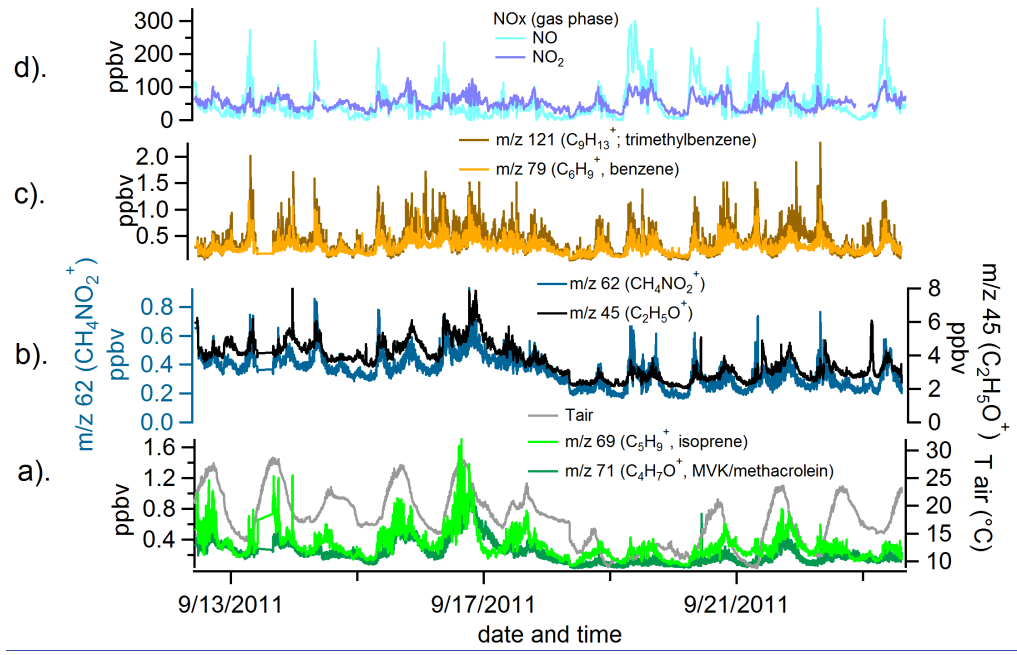

Helen Langley DeWitt 2/28/15 2:35 PM
Formatted: Tabs: 1.71", Left + Not at 1.07"

Helen Langley DeWitt 2/28/15 2:35 PM
Moved (insertion) [16]

Figure 3
The concentration in ppbv of PTR-ToF-MS VOC species identified isoprene and MVK/Methacrolin (left axis, A), VOC species associated with diesel exhaust ($CH_4NO_2^+$, $C_2H_5O^+$, B),VOC species associated with gasoline exhaust ($C_6H_7^+$, C_9H13^+, C). NO and NO_2 (gas-phase) ppbv concentrations (D) and ambient temperature (right axis, A) during the measurement period are also shown.

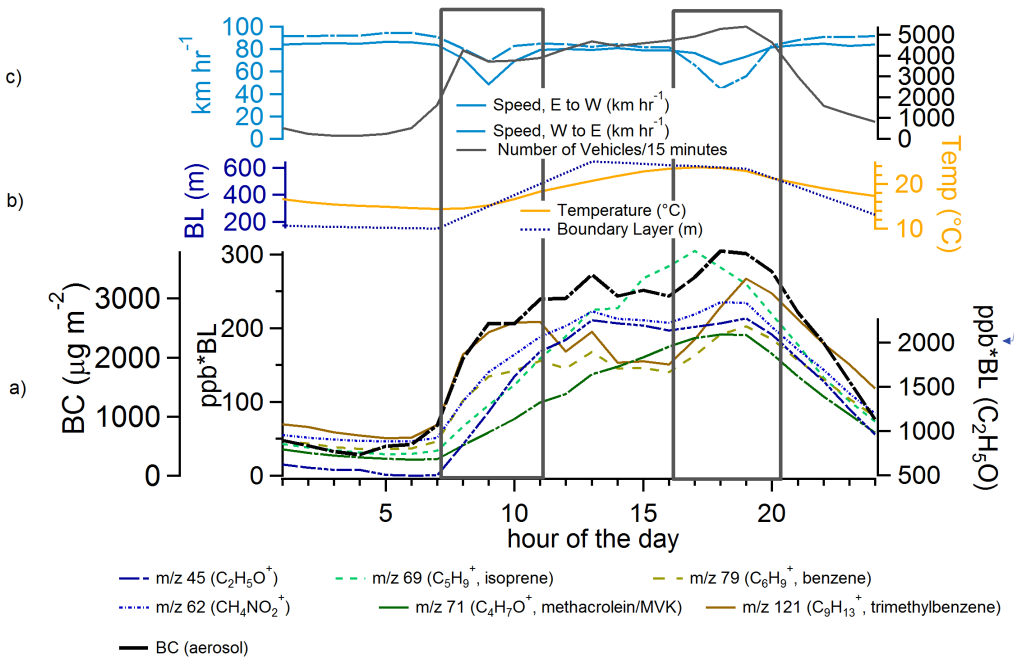

Figure 4 Diurnal profiles of boundary-layer scaled VOC peaks from PTR-MS measurements and BC peaks from MAAP measurements (A), temperature (right axis, B), boundary layer height (left axis, B), vehicular speed (left axis, C) and vehicle concentration (right axis, C).

Helen Langley DeWitt 2/28/15 2:35 PM
Formatted: Tabs: 3.08", Left

Helen Langley DeWitt 2/28/15 2:35 PM
Moved (insertion) [17]

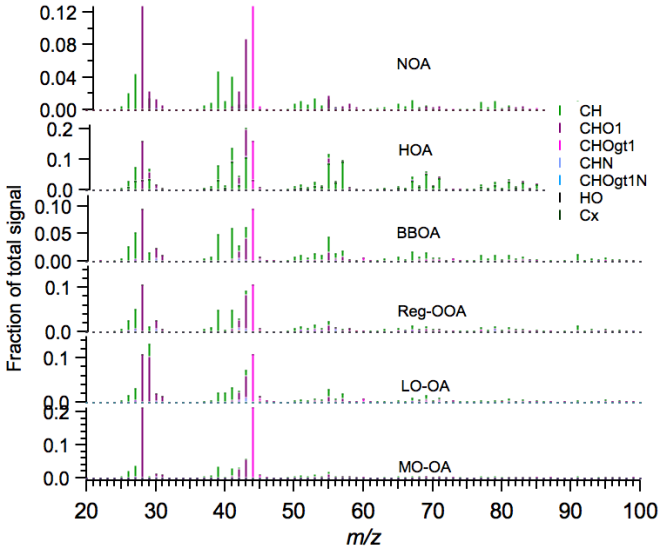

Figure 5:
The mass spectra of the six resolved factors, more oxidized organic aerosol (MO-OA), less oxidized organic aerosol (LO-OA), regional oxidized organic aerosol (reg-OOA), biomass burning organic aerosol (BBOA), hydrocarbon-like organic aerosol (HOA), and nitrogen-containing organic aerosol (NOA). Fraction of total signal is plotted against *m/z* and the peaks are color-coded to show their high-resolution identifications.

Helen Langley DeWitt 2/28/15 2:35 PM
Deleted: normalized LO-OA and

Helen Langley DeWitt 2/28/15 2:35 PM
Formatted: Widow/Orphan control, Hyphenate, Adjust space between Asian text and numbers, Font Alignment: Auto, Tabs:Not at 2.14"

Helen Langley DeWitt 2/28/15 2:35 PM
Deleted: (A) and HOA and LO-OA (B).

Helen Langley DeWitt 2/28/15 2:35 PM
Deleted: ... [35]

Helen Langley DeWitt 2/28/15 2:35 PM
Moved up [16]:

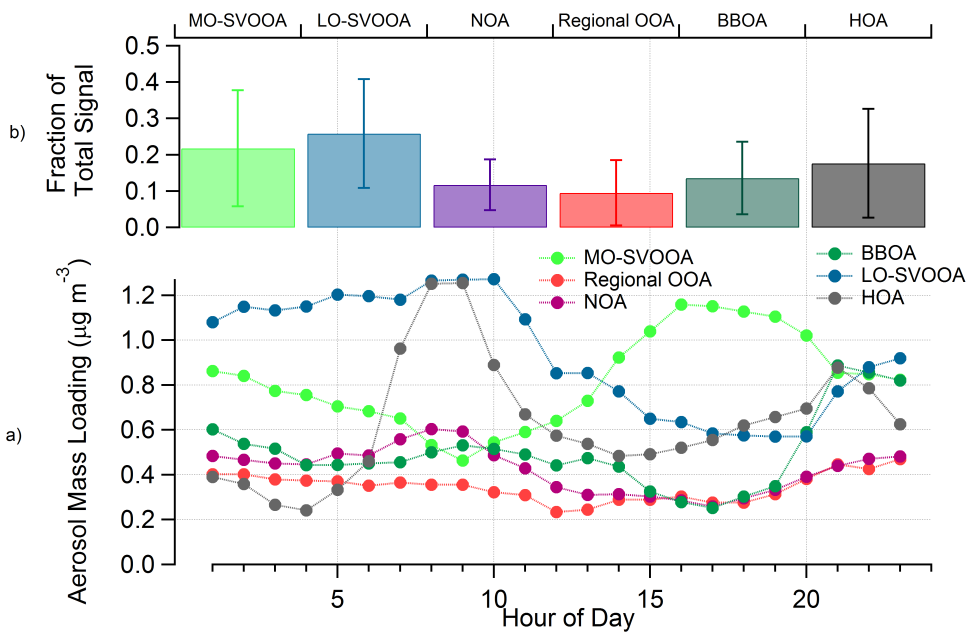

Figure 6: The diurnal profiles (A) and concentration and standard deviation of the six resolved aerosol factors (B).

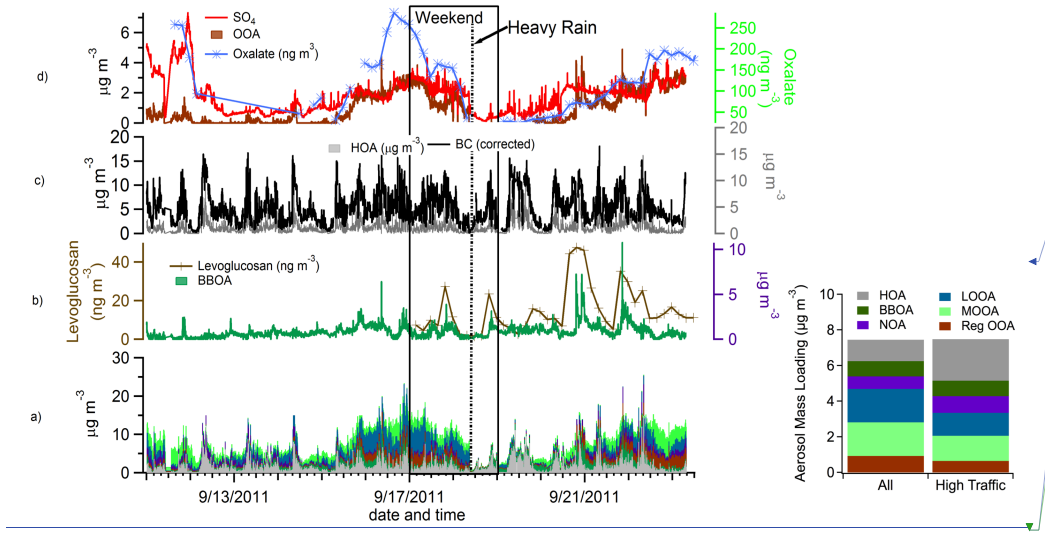

Figure 7:

The time series of the six-factor PMF solution (A), the resolved BBOA factor time series concentration (right axis, B) and off-line levoglucosan measurements (left axis, B), the resolved HOA factor time series concentration and BC (right axis, C), HR-TOF-AMS-measured SO_4 and the resolved regional OOA factor (left axis, D) and off-line oxalate measurements (right axis, right). The inset shows the calculated mass contribution during all (left) and high traffic (right) periods of each resolved PMF factor.

Helen Langley DeWitt 2/28/15 2:35 PM
Deleted: 12

Helen Langley DeWitt 2/28/15 2:35 PM
Formatted: Tabs:Not at 3.08"

Helen Langley DeWitt 2/28/15 2:35 PM
Moved (insertion) [18]

Helen Langley DeWitt 2/28/15 2:35 PM
Formatted: Widow/Orphan control, Hyphenate, Adjust space between Asian text and numbers, Font Alignment: Auto, Tabs:Not at 3.08"

Helen Langley DeWitt 2/28/15 2:35 PM
Formatted: Level 1, Tabs:Not at 3.08"

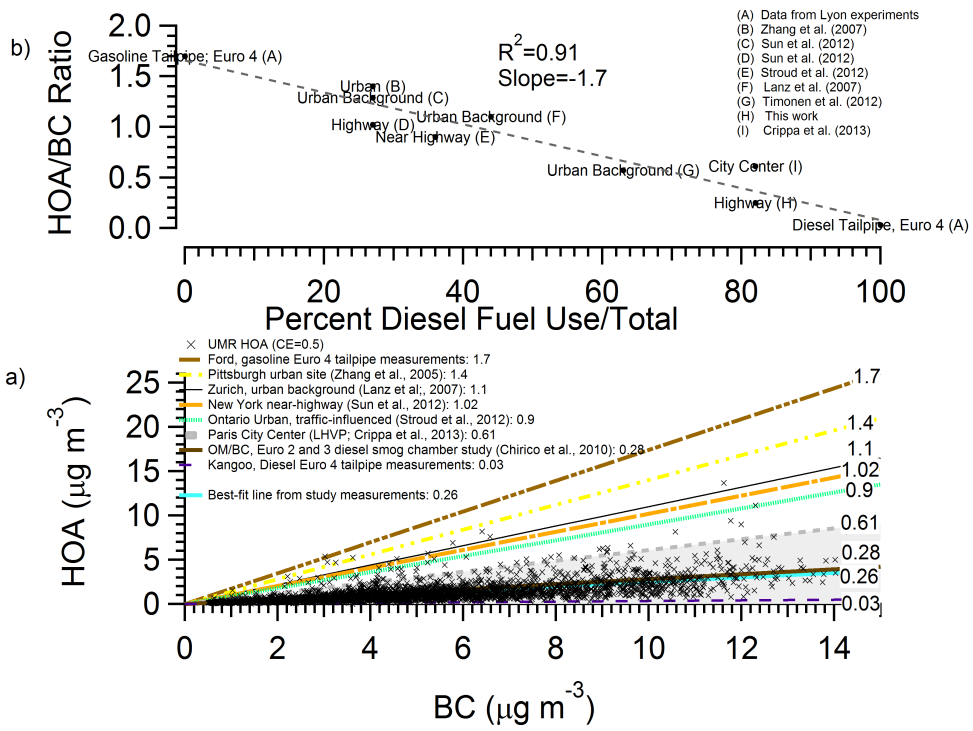

Figure 8
Calculated UMR HOA and measured BC concentrations from the campaign and HOA: BC ratios from previous field campaigns. Grey area is shaded to include a diesel-only environment and two French HOA: BC ratios: one from Crippa et al., (2013) and from this study (A). The HOA: BC ratio from various literature sources versus percent diesel fuel use out of total fuel use for the country of study (B).

Helen Langley DeWitt 2/28/15 2:35 PM
Formatted: Tabs: 1.07", Left + Not at 3.08"

Helen Langley DeWitt 2/28/15 2:35 PM
Deleted: . ... [36]

Helen Langley DeWitt 2/28/15 2:35 PM
Moved up [17]:

Helen Langley DeWitt 2/28/15 2:35 PM
Deleted: 13: Comparison of the

Helen Langley DeWitt 2/28/15 2:35 PM
Deleted: of different field campaigns and the diesel: gasoline fuel use in each of the respective measurement locations. HOA: BC ratios and locations from Figure 11, Percent diesel fuel use from the World Bank, (... [37]

Helen Langley DeWitt 2/28/15 2:35 PM
Moved up [18]:

Helen Langley DeWitt 2/28/15 2:35 PM
Deleted: 15: Daily concentration of carbon, BC, Fossil C, HOA C, and Modern C (A); Total organic carbon, HOA carbon, and SOA carbon

Helen Langley DeWitt 2/28/15 2:35 PM
Deleted: fossil organic carbon

Helen Langley DeWitt 2/28/15 2:35 PM
Formatted: Level 1, Tabs: 1.07", Left

Helen Langley DeWitt 2/28/15 2:35 PM
Formatted: Font:12 pt

Helen Langley DeWitt 2/28/15 2:35 PM
Formatted: Tabs: 3.08", Left

Helen Langley DeWitt 2/28/15 2:35 PM
Formatted: Font:18 pt

Helen Langley DeWitt 2/28/15 2:35 PM
Formatted: Tabs: 1.99", Left

Helen Langley DeWitt 2/28/15 2:35 PM
Formatted: Font:12 pt

Helen Langley DeWitt 2/28/15 2:35 PM
Formatted: Widow/Orphan control, Hyphenate, Adjust space between Asian text and numbers, Font Alignment: Auto

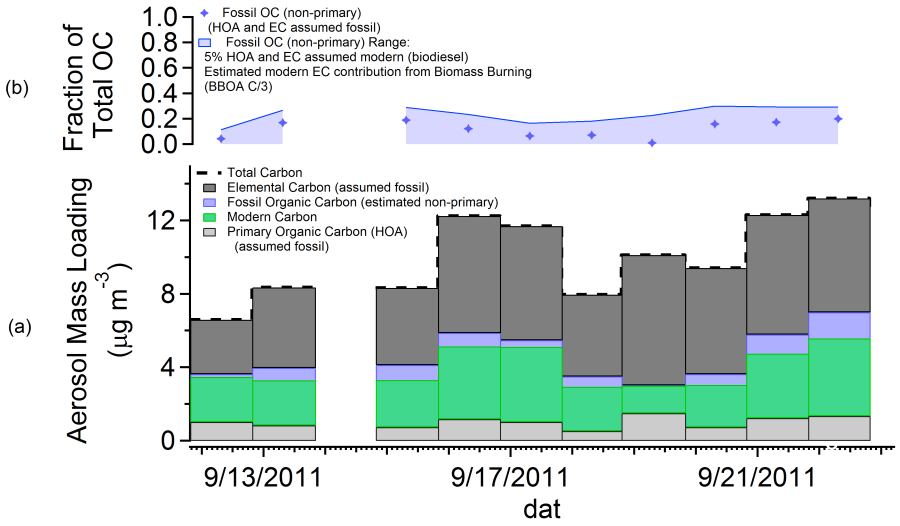

Figure 9: Measured EC and OC, with calculated contribution of non-primary fossil organic carbon (assuming 100% fossil EC and HOA, a) and assuming partial modern organic carbon EC and HOA contribution (b). The possible fossil OOA (light blue) was calculated by the subtraction of HOA from the fossil-OC fraction (assuming HOA either all fossil, A, or 95% fossil, B, and EC either all fossil (a) or 5%+BBOA/3 modern (b).

Helen Langley DeWitt 2/28/15 2:35 PM
Formatted: Widow/Orphan control, Hyphenate, Adjust space between Asian text and numbers, Font Alignment: Auto

Helen Langley DeWitt 2/28/15 2:35 PM
Formatted: Font:12 pt

References

Aiken, a. C., Salcedo, D., Cubison, M. J., Huffman, J. a., DeCarlo, P. F., Ulbrich, I. M., Docherty, K. S., Sueper, D., Kimmel, J. R., Worsnop, D. R., Trimborn, a., Northway, M., Stone, E. a., Schauer, J. J., Volkamer, R., Fortner, E., de Foy, B., Wang, J., Laskin, a., Shutthanandan, V., Zheng, J., Zhang, R., Gaffney, J., Marley, N. a., Paredes-Miranda, G., Arnott, W. P., Molina, L. T., Sosa, G. and Jimenez, J. L.: Mexico City aerosol analysis during MILAGRO using high resolution aerosol mass spectrometry at the urban supersite (T0) – Part 1: Fine particle composition and organic source apportionment, Atmos. Chem. Phys. Discuss., 9(2), 8377–8427, doi:10.5194/acpd-9-8377-2009, 2009.

Aiken, A. C., Decarlo, P. F., Kroll, J. H., Worsnop, D. R., Huffman, J. A., Docherty, K. S., Ulbrich, I. M., Mohr, C., Kimmel, J. R., Sueper, D., Sun, Y., Zhang, Q., Trimborn, A., Northway, M., Ziemann, P. J., Canagaratna, M. R., Onasch, T. B., Alfarra, M. R., Prevot, A. S. H., Dommen, J., Duplissy, J., Metzger, A., Baltensperger, U. and Jimenez, J. L.: O/C and OM/OC ratios of primary, secondary, and ambient organic aerosols with high-resolution time-of-flight aerosol mass spectrometry., Environ. Sci. Technol., 42(12), 4478–85 [online] Available from: http://www.ncbi.nlm.nih.gov/pubmed/18605574, 2008.

Bahreini, R., Middlebrook, a. M., de Gouw, J. a., Warneke, C., Trainer, M., Brock, C. a., Stark, H., Brown, S. S., Dube, W. P., Gilman, J. B., Hall, K., Holloway, J. S., Kuster, W. C., Perring, a. E., Prevot, a. S. H., Schwarz, J. P., Spackman, J. R., Szidat, S., Wagner, N. L., Weber, R. J., Zotter, P. and Parrish, D. D.: Gasoline emissions dominate over diesel in formation of secondary organic aerosol mass, Geophys. Res. Lett., 39(6), n/a–n/a, doi:10.1029/2011GL050718, 2012.

Birch, M. E. (Department of H. and H. S. and Cary, R. A. (Department of H. and H. S.: Elemental Carbon-Based Method for Monitoring Occupational Exposures to Particulate Diesel Exhaust, Aerosol Sci. Technol., 25(3), 221–241, 1996.

Bond, T. C., Doherty, S. J., Fahey, D. W., Forster, P. M., Berntsen, T., DeAngelo, B. J., Flanner, M. G., Ghan, S., Kärcher, B., Koch, D., Kinne, S., Kondo, Y., Quinn, P. K., Sarofim, M. C., Schultz, M. G., Schulz, M., Venkataraman, C., Zhang, H., Zhang, S., Bellouin, N., Guttikunda, S. K., Hopke, P. K., Jacobson, M. Z., Kaiser, J. W., Klimont, Z., Lohmann, U., Schwarz, J. P., Shindell, D., Storelvmo, T., Warren, S. G. and Zender, C. S.: Bounding the role of black carbon in the climate system: A scientific assessment, J. Geophys. Res. Atmos., 118(11), 5380–5552, doi:10.1002/jgrd.50171, 2013.

Broderick, B. . and Marnane, I. .: A comparison of the C2–C9 hydrocarbon compositions of vehicle fuels and urban air in Dublin, Ireland, Atmos. Environ., 36(6), 975–986, doi:10.1016/S1352-2310(01)00472-1, 2002.

Brugge, D., Durant, J. L. and Rioux, C.: Near-highway pollutants in motor vehicle exhaust: a review of epidemiologic evidence of cardiac and pulmonary health risks., Environ. Health, 6, 23, doi:10.1186/1476-069X-6-23, 2007.

Bruns, E. a, Perraud, V., Zelenyuk, A., Ezell, M. J., Johnson, S. N., Yu, Y., Imre, D., Finlayson-Pitts, B. J. and Alexander, M. L.: Comparison of FTIR and particle mass spectrometry for the measurement of particulate organic nitrates., Environ. Sci. Technol., 44(3), 1056–61, doi:10.1021/es9029864, 2010.

Carlton, a. G., Wiedinmyer, C. and Kroll, J. H.: A review of Secondary Organic Aerosol (SOA) formation from isoprene, Atmos. Chem. Phys. Discuss., 9(2), 8261–8305, doi:10.5194/acpd-9-8261-2009, 2009.

1735 Cavalli, F., Viana, M., Yttri, K. E., Genberg, J. and Putaud, J.-P.: Toward a standardised thermal-optical
1736 protocol for measuring atmospheric organic and elemental carbon: the EUSAAR protocol, Atmos. Meas. Tech.,
1737 3(1), 79–89 [online] Available from: http://www.atmos-meas-tech.net/3/79/ (Accessed 4 July 2014), 2010.

1738 Chameides, W., Lindsay, R., Richardson, J. and Kiang, C.: The role of biogenic hydrocarbons in urban
1739 photochemical smog: Atlanta as a case study, Science (80-.)., 241(4872), 1473–1475,
1740 doi:10.1126/science.3420404, 1988.

1741 Chen, J., Zhao, C. S., Ma, N. and Yan, P.: Aerosol hygroscopicity parameter derived from the light scattering
1742 enhancement factor measurements in the North China Plain, Atmos. Chem. Phys., 14(15), 8105–8118,
1743 doi:10.5194/acp-14-8105-2014, 2014.

1744 Cheung, K.L., Ntziachristos, L.,Tzamkiozis, T., Schauer, J.J., Samaras, Z., Moore, K.F. & Sioutas, C. (2010)
1745 Emissions of Particulate Trace Elements, Metals and Organic Species from Gasoline, Diesel, and Biodiesel Pas-
1746 senger Vehicles and Their Relation to Oxidative Potential, Aerosol Science and Technology, 44:7, 500-513,
1747 DOI: 10.1080/02786821003758294

1748 Chirico, R., Decarlo, P. F., Heringa, M. F., Tritscher, T., Richter, R. and Pr, A. S. H.: and Physics Impact of
1749 aftertreatment devices on primary emissions and secondary organic aerosol formation potential from in-use
1750 diesel vehicles : results from smog chamber experiments, , 3(Euro 4), 11545–11563, doi:10.5194/acp-10-11545-
1751 2010, 2010.

1752 Crippa, M., DeCarlo, P. F., Slowik, J. G., Mohr, C., Heringa, M. F., Chirico, R., Poulain, L., Freutel, F., Sciare,
1753 J., Cozic, J., Di Marco, C. F., Elsasser, M., Nicolas, J. B., Marchand, N., Abidi, E., Wiedensohler, a., Drewnick,
1754 F., Schneider, J., Borrmann, S., Nemitz, E., Zimmermann, R., Jaffrezo, J.-L., Prévôt, a. S. H. and Baltensperger,
1755 U.: Wintertime aerosol chemical composition and source apportionment of the organic fraction in the
1756 metropolitan area of Paris, Atmos. Chem. Phys., 13(2), 961–981, doi:10.5194/acp-13-961-2013, 2013.

1757 Decarlo, P. F., Kimmel, J. R., Trimborn, A., Northway, M. J., Jayne, J. T., Aiken, A. C., Gonin, M., Fuhrer, K.,
1758 Horvath, T., Docherty, K. S., Worsnop, D. R. and Jimenez, J. L.: Aerosol Mass Spectrometer, , 78(24), 8281–
1759 8289, doi:8410.1029/2001JD001213.Analytical, 2006.

1760 Docherty, K. S., Stone, E. A., Ulbrich, I. M., DeCarlo, P. F., Snyder, D. C., Schauer, J. J., Peltier, R. E., Weber,
1761 R. J., Murphy, S. M., Seinfeld, J. H., Grover, B. D., Eatough, D. J. and Jimenez, J. L.: Apportionment of Primary
1762 and Secondary Organic Aerosols in Southern California during the 2005 Study of Organic Aerosols in Riverside
1763 (SOAR-1), Environ. Sci. Technol., 42(20), 7655–7662, doi:10.1021/es8008166, 2008.

1764 El Haddad, I., Marchand, N., Dron, J., Temime-Roussel, B., Quivet, E., Wortham, H., Jaffrezo, J. L., Baduel, C.,
1765 Voisin, D., Besombes, J. L. and Gille, G.: Comprehensive primary particulate organic characterization of
1766 vehicular exhaust emissions in France, Atmos. Environ., 43(39), 6190–6198,
1767 doi:10.1016/j.atmosenv.2009.09.001, 2009.

1768 El Haddad, I., Marchand, N., Wortham, H., Piot, C., Besombes, J.-L., Cozic, J., Chauvel, C., Armengaud, a.,
1769 Robin, D. and Jaffrezo, J.-L.: Primary sources of $PM_{2.5}$ organic aerosol in an industrial Mediterranean city,
1770 Marseille, Atmos. Chem. Phys., 11(5), 2039–2058, doi:10.5194/acp-11-2039-2011, 2011.

1771 El Haddad, I., D'Anna, B., Temime-Roussel, B., Nicolas, M., Boreave, A., Favez, O., Voisin, D., Sciare, J.,
1772 George, C., Jaffrezo, J.-L., Wortham, H., and Marchand, N.: Towards a better understanding of the origins,
1773 chemical composition and aging of oxygenated organic aerosols: case study of a Mediterranean industrialized
1774 environment, Marseille, Atmos. Chem. Phys., 13, 7875-7894, doi:10.5194/acp-13-7875-2013, 2013.

Helen Langley DeWitt 2/28/15 2:41 PM
Formatted: Normal

Helen Langley DeWitt 2/28/15 2:41 PM
Formatted: Font:Check spelling and grammar

1775 Farmer, D. K., Matsunaga, a, Docherty, K. S., Surratt, J. D., Seinfeld, J. H., Ziemann, P. J. and Jimenez, J. L.:
1776 Response of an aerosol mass spectrometer to organonitrates and organosulfates and implications for atmospheric
1777 chemistry., Proc. Natl. Acad. Sci. U. S. A., 107(15), 6670–5, doi:10.1073/pnas.0912340107, 2010.

1778 Favez, O., El Haddad, I., Piot, C., Boréave, a., Abidi, E., Marchand, N., Jaffrezo, J.-L., Besombes, J.-L.,
1779 Personnaz, M.-B., Sciare, J., Wortham, H., George, C. and D'Anna, B.: Inter-comparison of source
1780 apportionment models for the estimation of wood burning aerosols during wintertime in an Alpine city
1781 (Grenoble, France), Atmos. Chem. Phys., 10(12), 5295–5314, doi:10.5194/acp-10-5295-2010, 2010.

1782 Fry, J. L., Draper, D. C., Zarzana, K. J., Campuzano-Jost, P., Day, D. a., Jimenez, J. L., Brown, S. S., Cohen, R.
1783 C., Kaser, L., Hansel, a., Cappellin, L., Karl, T., Hodzic Roux, a., Turnipseed, a., Cantrell, C., Lefer, B. L. and
1784 Grossberg, N.: Observations of gas- and aerosol-phase organic nitrates at BEACHON-RoMBAS 2011, Atmos.
1785 Chem. Phys., 13(17), 8585–8605, doi:10.5194/acp-13-8585-2013, 2013.

1786 Gentner, D. R., Isaacman, G., Worton, D. R., Chan, A. W. H., Dallmann, T. R., Davis, L., Liu, S., Day, D. a,
1787 Russell, L. M., Wilson, K. R., Weber, R., Guha, A., Harley, R. a and Goldstein, A. H.: Elucidating secondary
1788 organic aerosol from diesel and gasoline vehicles through detailed characterization of organic carbon emissions.,
1789 Proc. Natl. Acad. Sci. U. S. A., 109(45), 18318–23, doi:10.1073/pnas.1212272109, 2012.

1790 Goldstein, A. H., Koven, C. D., Heald, C. L. and Fung, I. Y.: Biogenic carbon and anthropogenic pollutants
1791 combine to form a cooling haze over the southeastern United States, Proc. Natl. Acad. Sci., 106(22), 8835–8840,
1792 doi:10.1073/pnas.0904128106, 2009.

1793 Hellebust, S., Temime-Roussel, B., Bertrand, A., Platt, S. M., El Haddad, I., Pieber, S., Zardini, A. A., Suarez-
1794 Bertoa, R., Slowik, J. G., Huang, R. J., Astorga, C., Prevot, A. S. H. and Marchand, N.: Comparison of Gasoline
1795 and Diesel Vehicles-Emission Factors of Volatile Organic Compounds from EURO5 Diesel and Gasoline
1796 Vehicles and Their Potential Integrated Influence on Air Quality, Am. Assoc. Aerosol Res., Fall 2013 , 2013.

1797 Hennigan, C. J., Sullivan, A. P., Collett, J. L. and Robinson, A. L.: Levoglucosan stability in biomass burning
1798 particles exposed to hydroxyl radicals, Geophys. Res. Lett., 37(9), n/a–n/a, doi:10.1029/2010GL043088, 2010.

1799 Herich, H., Gianini, M. F. D., Piot, C., Močnik, G., Jaffrezo, J.-L., Besombes, J.-L., Prévôt, A. S. H. and
1800 Hueglin, C.: Overview of the impact of wood burning emissions on carbonaceous aerosols and PM in large parts
1801 of the Alpine region, Atmos. Environ., 89, 64–75, doi:10.1016/j.atmosenv.2014.02.008, 2014.

1802 Hodzic, a., Jimenez, J. L., Madronich, S., Canagaratna, M. R., DeCarlo, P. F., Kleinman, L. and Fast, J.:
1803 Modeling organic aerosols in a megacity: potential contribution of semi-volatile and intermediate volatility
1804 primary organic compounds to secondary organic aerosol formation, Atmos. Chem. Phys., 10(12), 5491–5514,
1805 doi:10.5194/acp-10-5491-2010, 2010.

1806 Huffman, J. A., Jayne, J. T., Drewnick, F., Aiken, A. C., Onasch, T., Worsnop, D. R. and Jimenez, J. L.: Design,
1807 Modeling, Optimization, and Experimental Tests of a Particle Beam Width Probe for the Aerodyne Aerosol
1808 Mass Spectrometer, Aerosol Sci. Technol., 39(12), 1143–1163, doi:10.1080/02786820500423782, 2005.

1809 Hyvärinen, A.-P., Vakkari, V., L. Laakso, R. K. Hooda, Sharma, V. P., Panwar, T. S., Beukes, J. P., van Zyl, P.
1810 G., Josipovic, M., Garland, R. M., Andreae, M. O., Pöschl, U. and Petzold, A.: Correction for a measurement
1811 artifact of the Multi-Angle Absorption Photometer (MAAP) at high black carbon mass concentration levels,
1812 Atmos. Meas. Tech., 6(1), 81–90, doi:10.5194/amt-6-81-2013, 2013.

1813 Inomata, S., Tanimoto, H., Fujitani, Y., Sekimoto, K., Sato, K., Fushimi, A., Yamada, H., Hori, S., Kumazawa,
1814 Y., Shimono, A. and Hikida, T.: On-line measurements of gaseous nitro-organic compounds in diesel vehicle

exhaust by proton-transfer-reaction mass spectrometry, Atmos. Environ., 73(x), 195–203, doi:10.1016/j.atmosenv.2013.03.035, 2013.

Jaffrezo, J. L., Davidson, C. I., Kuhns, H. D., Bergin, M. H., Hillamo, R., Maenhaut, W., Kahl, J. W. and Harris, J. M.: Biomass burning signatures in the atmosphere of central TM High-density, , 103, 1998.

Jaffrezo, J.-L., Aymoz, G. and Cozic, J.: Size distribution of EC and OC in the aerosol of Alpine valleys during summer and winter, Atmos. Chem. Phys., 5(11), 2915–2925 [online] Available from: http://www.atmos-chem-phys.net/5/2915/2005/acp-5-2915-2005.html (Accessed 4 July 2014), 2005.

Janssen, N. A. H., World Health Organization, Regional Office for Europe and Joint WHO/Convention Task Force on the Health Aspects of Air Pollution: Health effects of black carbon. [online] Available from: http://www.euro.who.int/__data/assets/pdf_file/0004/162535/e96541.pdf, 2012.

Karner, A. A., Eisinger, D. S., and Niemeier, D. A. (2010). "Near-RoadwayAir Quality: Synthesizing the Findings from Real-World Data." Environ. Sci. and Tech, 44, 5334–5344.

Kroll, J. H., Ng, N. L., Murphy, S. M., Flagan, R. C. and Seinfeld, J. H.: Secondary organic aerosol formation from isoprene photooxidation under high-NO x conditions, Geophys. Res. Lett., 32(18), n/a–n/a, doi:10.1029/2005GL023637, 2005.

Lanz, V. A., Alfarra, M. R., Baltensperger, U., Buchmann, B., Hueglin, C. and Pr, A. S. H.: and Physics Source apportionment of submicron organic aerosols at an urban site by factor analytical modelling of aerosol mass spectra, , (2004), 1503–1522, 2007.

Lighty, J. S., Veranth, J. M. and Sarofim, A. F.: Combustion Aerosols: Factors Governing Their Size and Composition and Implications to Human Health, J. Air Waste Manage. Assoc., 50(9), 1565–1618, doi:10.1080/10473289.2000.10464197, 2000.

Liu, L., Lacis, A. a., Carlson, B. E., Mishchenko, M. I. and Cairns, B.: Assessing Goddard Institute for Space Studies ModelE aerosol climatology using satellite and ground-based measurements: A comparison study, J. Geophys. Res., 111(D20), D20212, doi:10.1029/2006JD007334, 2006.

Matthew, B. M., Middlebrook, A. M. and Onasch, T. B.: Collection Efficiencies in an Aerodyne Aerosol Mass Spectrometer as a Function of Particle Phase for Laboratory Generated Aerosols, Aerosol Sci. Technol., 42(11), 884–898, doi:10.1080/02786820802356797, 2008.

Minguillón, M. C., Perron, N., Querol, X., Szidat, S., Fahrni, S. M., Alastuey, A., Jimenez, J. L., Mohr, C., Ortega, A. M., Day, D. A., Lanz, V. A., Wacker, L., Reche, C., Cusack, M., Amato, F., Kiss, G., Hoffer, A., Decesari, S., Moretti, F., Hillamo, R., Teinilä, K., Seco, R., Peñuelas, J., Metzger, A., Schallhart, S., Müller, M., Hansel, A., Burkhart, J. F., Baltensperger, U., and Prévôt, A. S. H.: Fossil versus contemporary sources of fine elemental and organic carbonaceous particulate matter during the DAURE campaign in Northeast Spain, Atmos. Chem. Phys., 11, 12067-12084, doi:10.5194/acp-11-12067-2011, 2011.

Mohr, C., Huffman, J. A., Cubison, M. J., Aiken, A. C., Kenneth, S., Kimmel, J. R., Ulbrich, I. M., Hannigan, M. and Jimenez, J. L.: Characterization of Primary Organic Aerosol Emissions from Meat Cooking , Trash Burning , and Motor Vehicles with High-Resolution Aerosol Mass Spectrometry and Comparison with Ambient and Chamber Observations Characterization of Primary Organic Aerosol Em,, 2009.

Ng, N. L., Kroll, J. H., Chan, A. W. H., Chhabra, P. S., Flagan, R. C. and Seinfeld, J. H.: and Physics Secondary organic aerosol formation from m -xylene , toluene , and benzene, , (3), 3909–3922, 2007a.

Helen Langley DeWitt 2/28/15 2:42 PM
Formatted: Normal

Helen Langley DeWitt 2/28/15 2:42 PM
Formatted: Check spelling and grammar

1854 Ng, N. L., Kroll, J. H., Chan, A. W. H., Chhabra, P. S., Flagan, R. C. and Seinfeld, J. H.: and Physics Secondary
1855 organic aerosol formation from m -xylene , toluene , and benzene, , (3), 3909–3922, 2007b.

1856 Ng, N. L., Kwan, A. J., Surratt, J. D., Chan, A. W. H., Chhabra, P. S., Sorooshian, A., Pye, H. O. T., Crounse, J.
1857 D., Wennberg, P. O., Flagan, R. C. and Seinfeld, J. H.: Secondary organic aerosol (SOA) formation from
1858 reaction of isoprene with nitrate radicals (NO_3), Atmos. Chem. Phys., 8(14), 4117–4140, doi:10.5194/acp-8-
1859 4117-2008, 2008.

1860 Nordin, E. Z., Eriksson, a. C., Roldin, P., Nilsson, P. T., Carlsson, J. E., Kajos, M. K., Hellén, H., Wittbom, C.,
1861 Rissler, J., Löndahl, J., Swietlicki, E., Svenningsson, B., Bohgard, M., Kulmala, M., Hallquist, M. and Pagels, J.
1862 H.: Secondary organic aerosol formation from idling gasoline passenger vehicle emissions investigated in a
1863 smog chamber, Atmos. Chem. Phys., 13(12), 6101–6116, doi:10.5194/acp-13-6101-2013, 2013.

1864 Parrish, D. D., Stohl, A., Forster, C., Atlas, E. L., Blake, D. R., Goldan, P. D., Kuster, W. C. and de Gouw, J. A.:
1865 Effects of mixing on evolution of hydrocarbon ratios in the troposphere, J. Geophys. Res. Atmos., 112(D10),
1866 n/a–n/a, doi:10.1029/2006JD007583, 2007.

1867 Platt, S. M., El Haddad, I., Zardini, a. a., Clairotte, M., Astorga, C., Wolf, R., Slowik, J. G., Temime-Roussel,
1868 B., Marchand, N., Ježek, I., Drinovec, L., Močnik, G., Möhler, O., Richter, R., Barmet, P., Bianchi, F.,
1869 Baltensperger, U. and Prévôt, a. S. H.: Secondary organic aerosol formation from gasoline vehicle emissions in a
1870 new mobile environmental reaction chamber, Atmos. Chem. Phys., 13(18), 9141–9158, doi:10.5194/acp-13-
1871 9141-2013, 2013.

1872 Polo-Rehn, L.: Caractérisation des polluants dus au transport routier : Apports méthodologiques et cas d'études
1873 en Rhône Alpes, PhD thesis, Grenoble Univ., 2013.

1874 Presto, A. A., Miracolo, M. A., Donahue, N. M. and Robinson, A. L.: Secondary Organic Aerosol Formation
1875 from High-NOx Photo-Oxidation of Low Volatility Precursors: n-Alkanes, Environ. Sci. Technol., 44(6), 2029–
1876 2034, doi:10.1021/es903712r, 2010.

1877 Russell, L. M., Bahadur, R. and Ziemann, P. J.: Identifying organic aerosol sources by comparing functional
1878 group composition in chamber and atmospheric particles., Proc. Natl. Acad. Sci. U. S. A., 108(9), 3516–21,
1879 doi:10.1073/pnas.1006461108, 2011.

1880 Saarikoski, S., Carbone, S., Decesari, S., Giulianelli, L., Angelini, F., Canagaratna, M., Ng, N. L., Trimborn, a.,
1881 Facchini, M. C., Fuzzi, S., Hillamo, R. and Worsnop, D.: Chemical characterization of springtime
1882 submicrometer aerosol in Po Valley, Italy, Atmos. Chem. Phys., 12(18), 8401–8421, doi:10.5194/acp-12-8401-
1883 2012, 2012.

1884 Shilling, J. E., Zaveri, R. a., Fast, J. D., Kleinman, L., Alexander, M. L., Canagaratna, M. R., Fortner, E., Hubbe,
1885 J. M., Jayne, J. T., Sedlacek, a., Setyan, a., Springston, S., Worsnop, D. R. and Zhang, Q.: Enhanced SOA
1886 formation from mixed anthropogenic and biogenic emissions during the CARES campaign, Atmos. Chem.
1887 Phys., 13(4), 2091–2113, doi:10.5194/acp-13-2091-2013, 2013.

1888 Stroud, C. a., Moran, M. D., Makar, P. a., Gong, S., Gong, W., Zhang, J., Slowik, J. G., Abbatt, J. P. D., Lu, G.,
1889 Brook, J. R., Mihele, C., Li, Q., Sills, D., Strawbridge, K. B., McGuire, M. L. and Evans, G. J.: Evaluation of
1890 chemical transport model predictions of primary organic aerosol for air masses classified by particle component-
1891 based factor analysis, Atmos. Chem. Phys., 12(18), 8297–8321, doi:10.5194/acp-12-8297-2012, 2012.

1892 Sun, Y. L., Zhang, Q., Schwab, J. J., Chen, W.-N., Bae, M.-S., Hung, H.-M., Lin, Y.-C., Ng, N. L., Jayne, J.,
1893 Massoli, P., Williams, L. R. and Demerjian, K. L.: Characterization of near-highway submicron aerosols in New

1894 York City with a high-resolution aerosol mass spectrometer, Atmos. Chem. Phys., 12(4), 2215–2227,
1895 doi:10.5194/acp-12-2215-2012, 2012.

1896 Sun, Y., Zhang, Q., Zheng, M., Ding, X., Edgerton, E. S. and Wang, X.: Characterization and source
1897 apportionment of water-soluble organic matter in atmospheric fine particles (PM2.5) with high-resolution
1898 aerosol mass spectrometry and GC-MS., Environ. Sci. Technol., 45(11), 4854–61, doi:10.1021/es200162h,
1899 2011.

1900 Thornhill, D. a., Williams, a. E., Onasch, T. B., Wood, E., Herndon, S. C., Kolb, C. E., Knighton, W. B., Zavala,
1901 M., Molina, L. T. and Marr, L. C.: Application of positive matrix factorization to on-road measurements for
1902 source apportionment of diesel- and gasoline-powered vehicle emissions in Mexico City, Atmos. Chem. Phys.,
1903 10(8), 3629–3644, doi:10.5194/acp-10-3629-2010, 2010.

1904 Ulbrich, I. M., Canagaratna, M. R., Zhang, Q., Worsnop, D. R. and Jimenez, J. L.: Interpretation of organic
1905 components from Positive Matrix Factorization of aerosol mass spectrometric data, Atmos. Chem. Phys., 9(9),
1906 2891–2918, doi:10.5194/acp-9-2891-2009, 2009.

1907 Vestreng, V., Ntziachristos, L., Semb, A., Reis, S., Isaksen, I. S. A. and Tarras, L.: and Physics Evolution of NO
1908 x emissions in Europe with focus on road transport control measures, , (x), 1503–1520, 2009.

1909 WHO: Health Effects of Particulate Matter: Policy imlications for countries in eastern Europe, Caucasus and
1910 central Asia, World Heal. Organ., 15 [online] Available from: www.euro.who.int, 2013.

1911 World Bank: World Development Report 2011: World Development Indicators, Fossil Fuel Energy
1912 Consumption., 2011.

1913 Xu, J., Zhang, Q., Chen, M., Ge, X., Ren, J. and Qin, D.: Chemical composition, sources, and processes of urban
1914 aerosols during summertime in Northwest China: insights from High Resolution Aerosol Mass Spectrometry,
1915 Atmos. Chem. Phys. Discuss., 14(11), 16187–16242, doi:10.5194/acpd-14-16187-2014, 2014.

1916 Zhang, Q., Worsnop, D. R., Canagaratna, M. R. and Jimenez, J.-L.: Hydrocarbon-like and oxygenated organic
1917 aerosols in Pittsburgh: insights into sources and processes of organic aerosols, Atmos. Chem. Phys. Discuss.,
1918 5(5), 8421–8471, doi:10.5194/acpd-5-8421-2005, 2005.

1919
1920
1921